Zoomorphology (2019) 138:137–158
https://doi.org/10.1007/s00435-018-0420-0

ORIGINAL PAPER

Musculoskeletal development of the Central African caecilian *Idiocranium russeli* (Amphibia: Gymnophiona: Indotyphlidae) and its bearing on the re-evolution of larvae in caecilian amphibians

Tobias Theska[1] · Mark Wilkinson[2] · David J. Gower[2] · Hendrik Müller[1,2]

Received: 29 June 2018 / Revised: 22 September 2018 / Accepted: 28 September 2018 / Published online: 12 October 2018

Abstract
Few detailed accounts of the developmental morphology of caecilian amphibians exist and recent studies have highlighted problems concerning the homology of some skull elements. We investigated the embryonic and post-hatching development of the skeleton and musculature of *Idiocranium russeli*, a possibly miniaturized caecilian endemic to Cameroon. *Idiocranium* has been suggested to be direct developing; our results strongly support this hypothesis. The external morphology of different embryonic stages, the ossification sequence, and the configuration of the cranial muscles of *I. russeli* indicate heterochronic shifts of adult traits into embryonic development, as well as the loss or absence of various larval and metamorphic traits. For example, the tentacle, which plesiomorphically develops during metamorphosis, is already fully developed in late embryos. The maxilla and the palatine, which fuse to form the maxillopalatine (during metamorphosis in most biphasic species), fuse well before hatching. Muscles exclusive to the larva, such as the m. interhyoideus and m. hyomandibularis, are absent during development, whereas adult muscles including the m. genioglossus and m. cephalodorsosubpharyngeus, form during embryonic development. A larval ceratobranchial IV is present and fuses to the ceratobranchial III very early in ontogeny. In its near complete absence of larval traits during development, *I. russeli* resembles the Indian indotyphlid *Gegeneophis ramaswamii*; this similarity complicates a straightforward explanation for the re-evolution of free-living larvae in Seychelles indotyphlid caecilians.

Keywords Morphology · Ontogeny · Larval re-evolution · Life history · Ossification sequence

Introduction

Extant amphibians (Lissamphibia) comprise three orders: caecilians (Gymnophiona), frogs and toads (Anura), and newts and salamanders (Caudata). Caecilians, the least speciose of the three orders, comprise 209 extant species classified in 10 families (Wilkinson et al. 2011; Kamei et al. 2012; Frost 2018). Caecilians are the sister group of Batrachia (Anura + Caudata) (e.g., Szarski 1962; Parsons and Williams 1963; Milner 1988; San Mauro 2010) but differ from the more familiar batrachians in many respects. Caecilians are elongate, snake-like amphibians that lack any trace of limbs or girdles. Most are terrestrial as adults, with surface cryptic and/or burrowing lifestyles. This is reflected in their morphology; all caecilians have a more or less heavily ossified and compact skull quite unlike those of frogs and salamanders (Taylor 1969; Wake 2003). Another unique caecilian feature is the tentacle, a likely mechano- and chemosensory organ that forms from the eyelid and its associated components (Billo and Wake 1987; Himstedt 1996).

Caecilians are poorly known and one of the least studied major clades of tetrapods (e.g., Himstedt 1996; Kleinteich 2009; Wilkinson 2012; San Mauro et al. 2014). Plesiomorphically, caecilians have a biphasic life cycle with a free-living, aquatic, or semi-aquatic larval stage as do other amphibians (Dunn 1942; San Mauro et al. 2014). As far as is known, caecilian larvae hatch from terrestrially deposited eggs. The duration of larval development before

✉ Tobias Theska
tobias.theska@tuebingen.mpg.de

✉ Hendrik Müller
hendrik.mueller@uni-jena.de

[1] Institut für Zoologie und Evolutionsforschung, Friedrich-Schiller-Universität Jena, Erbertstr. 1, 07743 Jena, Germany

[2] Department of Life Sciences, The Natural History Museum, SW7 5BD London, UK

metamorphosis into primarily terrestrial adults varies interspecifically (Himstedt 1996). However, most caecilians do not have a free-living larval stage and develop either directly or are viviparous. Within caecilians, direct development is thought to have evolved in stem-Teresomata, a clade comprising two-thirds of extant caecilian species (San Mauro et al. 2014). Direct development has evolved independently in all major living amphibian lineages (e.g., Wake and Hanken 1996; San Mauro et al. 2014; Schweiger et al. 2017). It is characterized by complete loss of the free-living and morphologically distinct larval stage. Embryonic development is subject to ontogenetic repatterning and a large-scale loss of larval characters that culminate in the hatching of a fully formed juvenile comparable to a postmetamorph of a biphasic developer (Hanken 2003). Although the evolution of direct development and terrestrial development in general is not well-understood, it usually is thought to have evolved in response to aquatic predation pressures, parasite avoidance, or some environmental factors (e.g., Magnusson and Hero 1991; Todd 2007; Müller et al. 2013; Liedtke et al. 2017).

Direct development has often been considered an evolutionary dead end (Wake and Hanken 1996), but several studies have inferred the reacquisition of a free-living, aquatic larva from a presumably terrestrial or direct-developing ancestor in marsupial frogs (Duellman et al. 1988; Wiens et al. 2007; Duellman 2015) and plethodontid salamanders (Chippindale et al. 2004; Mueller et al. 2004). The proposed re-evolution of an aquatic larva from a direct-developing ancestor in desmognathines caused some controversy (Bonett et al. 2005; Bruce 2005; Chippindale and Wiens 2005). However, Kerney et al. (2012) showed that some larval traits are maintained early in the ontogeny of direct-developing plethodontids; thus, the reappearance in larval developers may represent an elaboration of an existing developmental sequence, rather than de novo evolution of a previously lost phenotype. Re-evolution of a larva has also been proposed to have occurred within the Seychelles radiation of indotyphlid caecilians (San Mauro et al. 2014). Of the three genera and eight species of caecilians endemic to the Seychelles archipelago (Maddock et al. 2018), the species of *Hypogeophis* are known or presumed to be direct developing (Brauer 1899; Müller 2006), whereas *Grandisonia* and *Praslinia* have been reported to have free-living larvae (e.g., Parker 1958; Nussbaum 1984; Müller 2007). The Seychelles caecilians with free-living larvae are deeply nested in a clade of predominantly direct-developing caecilians (San Mauro et al. 2014; see also; Gower et al. 2008). Developmental data are available for the Seychelles *H. rostratus* and for the Indian indotyphlid *Gegeneophis ramaswamii*. The latter and its congeners, along with *Indotyphlus*, is part of the putative sister group of the Seychelles radiation. Both *H. rostratus* and *G. ramaswamii* are direct developers, with *H. rostratus* reported to express more larval-like characters than *G. ramaswamii* during embryonic development (Müller et al. 2005; Müller 2006). Based on the available data, we cannot ascertain what larval traits might have been retained in the ontogeny of the last common ancestor of the Seychelles and the Indo-Seychelles indotyphlid clades. Thus, we cannot determine which features might facilitate a re-elaboration of a larval phenotype as seen in *Praslinia* and *Grandisonia*.

We investigated the ontogeny of the cranial and mandibular skeleton and musculature in *Idiocranium russeli* (Parker 1936) in an effort to elucidate the developmental and life history diversity of indotyphlid caecilians. *Idiocranium russeli* apparently is a direct-developing species (Wake 1977; Gower et al. 2015) that is sister taxon of all other indotyphlids that have been included in molecular phylogenetic studies (San Mauro et al. 2014). It is a small, Central African caecilian (Gower et al. 2015) that has several unusual traits that are thought to have resulted from miniaturization (Wake 1986). Previous studies focussed on overall adult morphology or particular anatomical aspects of *I. russeli* (Parker 1936; Wake 1986; Maddin et al. 2012; de Bakker et al. 2015); relevant developmental data are not available. Herein, we explore whether larval traits are present in this presumably direct-developing species as a means to understand the potential pathways that led to the postulated re-evolution of free-living larvae within Indotyphlidae.

Materials and methods

Specimens

A total of 16 *I. russeli* including a range of life history stages (Table 1) was studied. The caecilians were collected near Tinta, Southwest Province, Cameroon, near the type locality of the species; see Gower et al. (2015) for further details. The specimens are deposited in the herpetological collections of the Natural History Museum, London, accessioned under BMNH 2008.688 and herein identified individually by field tag numbers (Table 1). Specimens were fixed in 5–10% formalin in the field and subsequently maintained in 70% industrial methylated spirit. We processed eight specimens of different ontogenetic stages for detailed examination to investigate musculoskeletal development; see Table 1 for details.

Staging and terminology

We followed established practice (Müller et al. 2005; Müller 2006; Pérez et al. 2009) and used the detailed descriptions of the external development of *H. rostratus* and *Grandisonia alternans* provided by Brauer (1899) as a staging reference; see Müller et al. (2005) for a detailed rationale. The

Table 1 Specimens of *Idiocranium russeli* examined for this study

Voucher	ID	Stage	TL (mm)	Preparation
MW08646	Idio1	40	17.7	Serial section
MW08375	Idio2	40	20.3	–
MW08459	Idio3	41	[a]	Cleared and stained
MW08645	Idio4	42	21.6	–
MW08372	Idio5	43	20	Serial section, 3D reconstruction
MW08644	Idio6	47/48	32.8	Cleared and stained
MW08694	Idio7	48	29.6	Serial section
MW08694	Idio8	50	30.5	–
MW08697	Idio9	50	30	–
MW08697	Idio10	50	31.3	–
MW08697	Idio11	50	33.3	Manual dissection, cleared and stained
MW08621	Idio12	50+	35	Serial section
MW08620	Idio13	50+	35	–
MW08620	Idio14	50+	36	–
MW08621	Idio15	50+	36.5	–
MW08621	Idio16	50+	37	Manual dissection, cleared and stained
MW08511	–	Adult	110	Female, µCT scanned

ID Identification number in this study, *TL* total length

[a]Not measured due to damaged body wall

terms "hatchling" or "juvenile" are applied to individuals that have hatched and are usually found associated with an adult, presumably their mother (Gower et al. 2015). These juveniles are designated here as Brauer Stage (BS) 50+ (Table 1). Terminology of skeletal elements follows that of Müller (2006) unless noted otherwise. Myological descriptions follow those of Kleinteich and Haas (2007, 2011) and innervation was verified when possible.

Preparation of specimens

We used a Stemi SV11 (Zeiss) stereomicroscope with an attached ColorView 3FV digital camera and the software AnalySIS to photograph specimens, and to measure total length (TL) digitally with the segmented lines tool of FIJI (ImageJ). Four specimens (Table 1) were double stained for bone and cartilage (Krings et al. 2017). Two hatchlings (Idio11 and Idio16; Table 1) were dissected manually after cartilage staining to inspect the musculature; to enhance contrast, we temporarily stained muscles with Lugol's solution. Drawings were prepared with the aid of a camera lucida attached to a SteREO Discovery.V12 (Zeiss) and processed using Adobe Illustrator CS6. Photos were taken with a SteREO Discovery.V12 (Zeiss) equipped with an AxioCam ICc (Zeiss) digital camera. Specimens selected for histology (Table 1) were post-fixed in 2.5% buffered formalin for 2 days and decapitated. Heads of young embryos (Idio1 and Idio5) were decalcified using ascorbic acid, while the heads of older specimens (Idio7 and Idio12) were decalcified with nitric acid. Specimens were embedded in paraffin, serially sectioned transversely at 7 µm using a MICROM HM3552; sections were stained with azocarmine red and aniline blue (AZAN) following standard protocols (Mulisch and Welsch 2015).

Alignment and 3D reconstruction

A three-dimensional reconstruction of the cranial, mandibular and hyobranchial skeleton was generated for one embryo (Idio5) from the histological sections. We digitised all sections using an Olympus BX51 microscope equipped with an Olympus XC10 digital camera. Photographs were taken at 20× magnification with a colour depth of 24-bit (RGB) and all images were then converted to 8-bit (greyscale) and the resolution reduced to 65 ppi with the batch-processing tool of Adobe Photoshop CS6. The resulting 400 images were aligned automatically using the TrakEM2 plugin in FIJI (ImageJ). The aligned image stack was cropped to a size of 3212×2972 p and imported into Amira 6.3.0, where the contours of all skeletal elements were segmented manually. The generated surfaces were exported to Autodesk Maya 2017 for final processing and image rendering. An adult specimen was scanned using a Metris X-Tek HMX ST 225 high-resolution X-ray computed tomography system. The reconstructed slices were rendered as a three-dimensional volume using VGStudio MAX v2.0 (Volume Graphics).

Results

External embryonic development

The external morphology of the developmental stages examined corresponds closely to Brauer's (1899) report. At Brauer Stage (BS) 40, slight anlagen of labial folds are visible on both sides of the head, where they extend rostrally from the angle of the mouth and taper out anterior to the nostrils. Tentacle anlagen are visible as small lateral pits at the margin of the upper lip, approximately midway between the nostril and the eye. Gill slits and components of the mechanosensory lateral line are seen neither at this stage in the sectioned specimen nor in later stages. BS 40 and 41 are similar in overall appearance, but in BS 41, the labial folds are indistinct and largely reduced, whereas the tentacle anlagen are larger. At BS 43, the tentacle is a small, globular structure in the anterolateral region of the snout, and labial folds are no longer visible. By BS 47/48, primary and secondary annuli are easily identified; two collars are present (the first being wider and longer than the second) and the tentacles are fully differentiated and erupted in a position comparable to the adult condition. At BS 50, when hatching occurs, external gills are completely absent and only the youngest and smallest individual of this stage (Idio11; Table 1) has a small scar on the left side where the external gills previously inserted. At BS 50, labial folds and gill slits are absent; the body terminus is rounded and a tail fin is absent.

Skeleton

Cranium

At BS 40, the youngest stage investigated (Table 1), chondrification is advanced; the palatoquadrate (pq), the otic capsule (oc), and occipital arch (oca) are the most prominent structures. The occipital arch is fused to the posterior end of the otic capsule dorsally and to the parachordal cartilage ventrally to form the foramen jugulare (fju; Fig. 1b). The walls of the otic capsule are relatively thin, especially medially (Fig. 1a, b). A bar-like basal plate (bp; hypochordal commissure of Duellman and Trueb 1986) connects the caudal parts of the parachordal cartilages medially (pac; Fig. 1b, c). It is pierced by the chorda dorsalis. A tectum synoticum, uniting the dorsal parts of the otic capsules medially, is absent. Anteriorly, the otic capsule is connected to the parachordal cartilage ventrally and to the taenia marginalis (tm) dorsally (Fig. 1). The parachordal cartilage and the taenia marginalis are cylindrical in cross section and oriented horizontally. The pila antotica (pao) is a vertical, bar-shaped cartilage that connects the anterior tip of the taenia marginalis dorsally to the parachordal cartilage ventrally (Fig. 1). At the level of the pila antotica, the anterior end of the taenia marginalis is contiguous with the posterior end of the orbital cartilage. Similarly, the ventral parachordal cartilage is contiguous with the trabecular cartilage (trc) anteriorly. Thus, the taenia marginalis and orbital cartilage form the dorsolateral bridge between the otic capsule and the ethmoidal region, and the parachordal and trabecular cartilages form the ventrolateral bridge (Fig. 1). The foramen palatinum (fpal) pierces the parachordal for the passage of the palatine branch of the facial nerve [VII] (Fig. 1c).

The pila preoptica (ppo) lies anterior to the pila antotica; it curves medially toward the midline of the endocranium to unite with its contralateral part and form the internasal plate (inp) (Fig. 1c). The entire ethmoidal region is poorly differentiated and only weakly chondrified at this stage. The posterior part of the septum nasi (sn) is formed by cartilage, but the rest of the rostral endocranium is composed of precartilaginous tissue. A slender, rod-like stapes (st) lies in the anterolateral part of the wide fenestra ovalis (fov). The stapes is Y-shaped in ventral view; the lateral process is directed anteriorly toward the caudal surface of the palatoquadrate, whereas the ventromedial process is directed toward the parachordal cartilage (Fig. 1a, c). There is no direct contact between the stapes and palatoquadrate and parachordal cartilage, except for some condensations of mesenchymal cells. The large palatoquadrate is oriented dorsoventrally and has a compact bar shape (Fig. 1a). Its articular surface for Meckel's cartilage is well-chondrified. A short, medially projecting processus pterygoideus (ppt; Fig. 1c) juts from the medial edge of the palatoquadrate. The vomer (vom) is a small ossification represented by a simple, transverse, and slightly curved bony lamella that lies ventral to the internasal plate. Additionally, there is a thin layer of perichondral bone around the occipital arch, forming the endoskeletal exoccipital (exo).

The cranial morphology of BS 41 embryos is generally similar to BS 40. However, the chondrification of the ethmoidal region is more advanced and the septum nasi and prenasal process (pp; an anterior extension of the septum nasi) are now completely formed by cartilage (Fig. 2a, b). The internasal plate is also fully chondrified and continuous with the vertical septum nasi along the midline of the plate (Fig. 1). The ventral and lateral portions of the rostral endocranium are still mostly represented by mesenchymal condensations (Fig. 2a, b). The stapes and palatoquadrate are large, appear more solidly chondrified, and lie closer to one another. The relative diameter of the dorsal fenestra of the otic capsule is smaller. The vomer is larger and the exoccipital now completely encircles the centre of the occipital arch (Fig. 2b). The premaxilla (pmx) is a

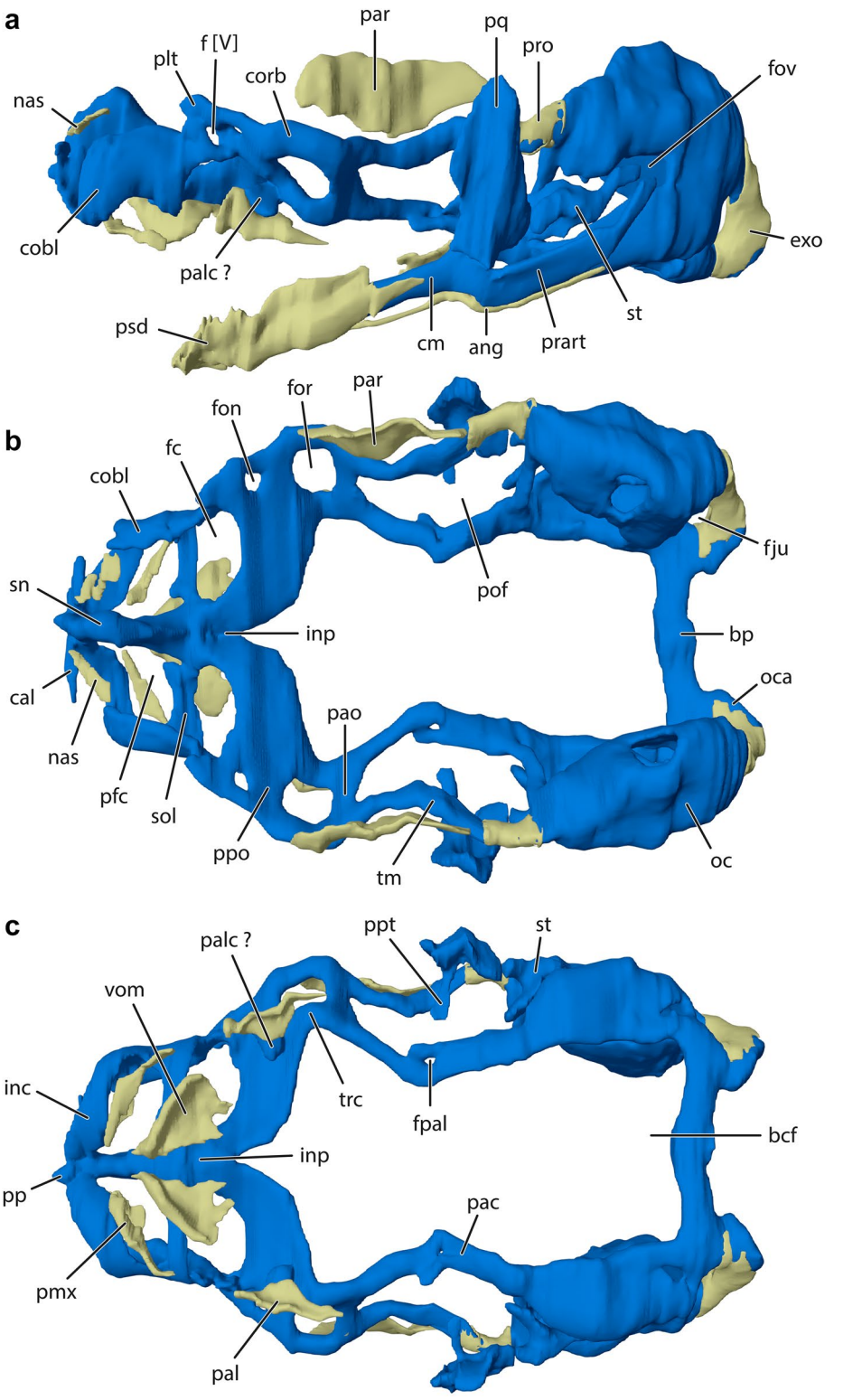

Fig. 1 Three-dimensional reconstruction of the embryonic cranial and mandibular skeleton of *Idiocranium russeli* at BS 43 in **a** lateral, **b** dorsal, and **c** ventral view. Lower jaw omitted in **b, c**. Cartilage blue, bone pale brown. *ang* angular, *bp* basal plate, *bcf* basicranial fenestra, *cal* alary cartilage, *cm* cartilago meckeli, *cobl* oblique cartilage, *corb* orbital cartilage, *exo* exoccipital, *f[V]* trigeminus foramen, *fc* choanal foramen, *fju* foramen jugulare, *fon* foramen orbitonasale, *for* foramen orbitale, *fov* fenestra ovalis, *fpal* palatine foramen, *inc* infranarial cartilage, *inp* internasal plate, *nas* nasal, *oc* otic capsule, *oca* occipital arch, *pac* parachordal cartilage, *pal* palatine, *pao* pila antotica, *palc* palatine cartilage, *par* parietal, *pfc* prechoanal foramen, *plt* planum terminale, *pmx* premaxilla, *pof* prootic foramen, *pp* prenasal process, *ppo* pila preoptica, *ppt* processus pterygoideus, *pq* palatoquadrate, *prart* processus retroarticularis, *pro* prooctics, *psd* pseudodentary, *sol* solum nasi, *sn* septum nasi, *st* stapes, *tm* taenia marginalis, *trc* trabecular cartilage, *vom* vomer. Scale bar 1 mm. (Color figure online)

short, horizontal rod anterior to the vomer (Fig. 2a, b), and the palatine (pal) is present as a long rod posterior to the vomer and ventral to the pila preoptica (Fig. 2a).

At BS 43, the walls of the otic capsule seem more robust and their dorsal openings are smaller than in previous stages. The stapes is larger than in BS 41 and fills most of

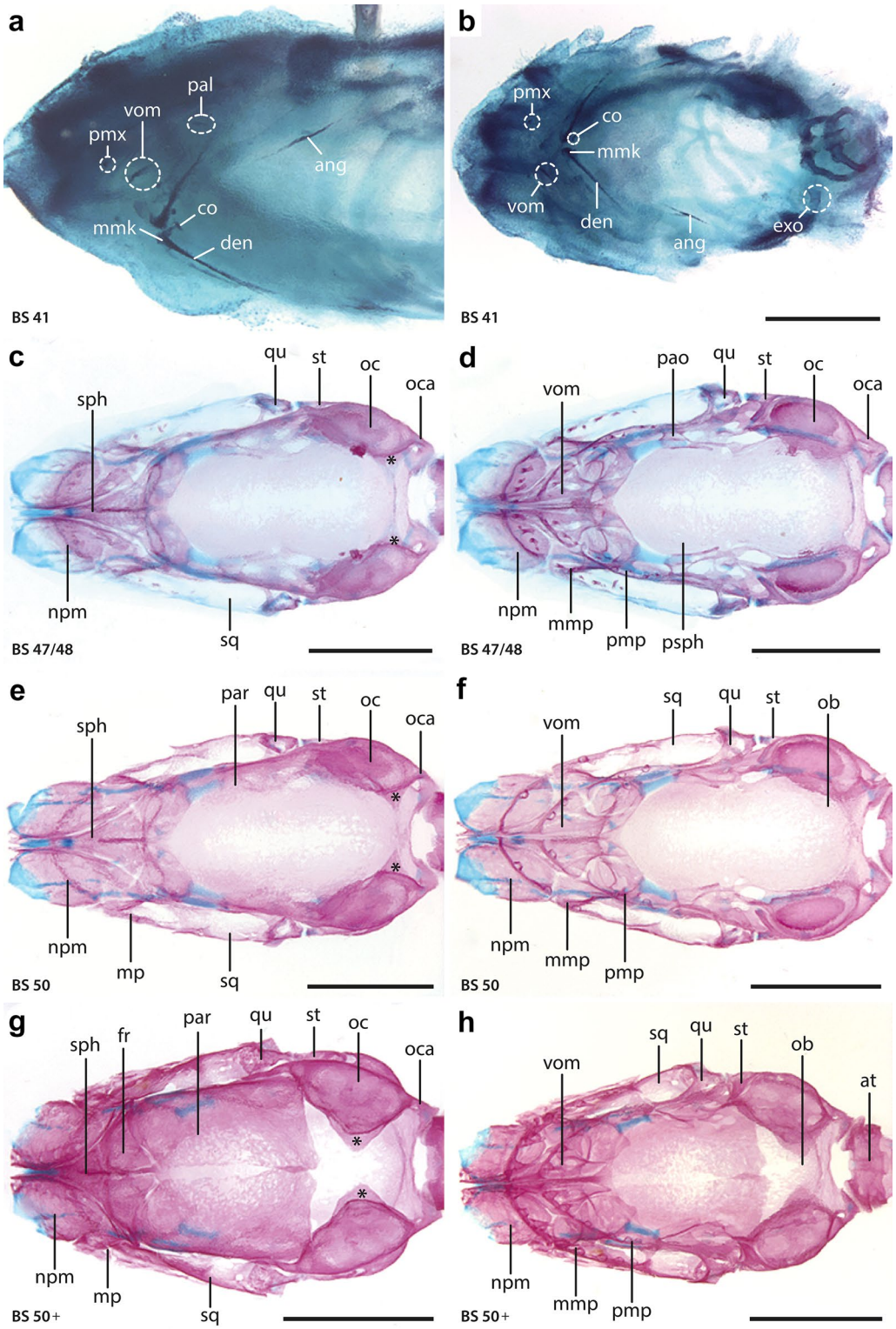

Fig. 2 Development of the skull in *Idiocranium russeli*. **a, b** Ventrolateral views of the head of Idio3 (BS 41). **c**–**h** Dorsal views (left) and ventral views (right) of the skulls of older embryos and juveniles. **c, d** Skull of Idio6 (BS 47/48). **e, f** Skull of Idio11 (BS 50). **g, h** Skull of Idio16 (BS 50+). Asterisk indicates intramembranous ossifications extending from the exoccipitals to form the dorsal margin of the foramen magnum. *ang* angular, *at* atlas, *co* coronoid, *den* dentary, *exo* exoccipital, *fr* frontal, *mmp* maxillar portion of the maxillopalatine, *mp* maxillopalatine, *npm* nasopremaxilla, *ob* os basale, *oc* otic capsule, *oca* otic arch, *pal* palatine, *pao* pila antotica, *par* parietal, *pmp* palatine portion of the maxillopalatine, *pmx* premaxilla, *psph* parasphenoid, *qu* quadrate, *sph* sphenethmoid, *sq* squamosal, *st* stapes, *vom* vomer. Scale bars 1 mm

the fenestra ovalis (Fig. 1a). Its lateral process articulates with the caudally projecting otic process of the palatoquadrate. None of the barely visible fusion marks between the parachordal and trabecular cartilages and between the taenia marginalis and the orbital cartilage (BS 40) is visible. The pila antotica and pila preoptica are more substantially chondrified. A rounded planum terminale (plt) forms part of the lateral wall of the rostral endocranium and the anterior border of the foramen orbitonasale (fon; Fig. 1a, b). Anterior to the foramen orbitonasale is a small foramen for the nervus trigeminus [V] (Fig. 1a). A thin solum nasi (sol) forms the floor of the nasal capsule anterior to the pila preoptica, as well as a weakly chondrified connection between the internasal plate and the oblique cartilage. It also forms the anterior margin of the choanal foramen (fc) and the posterior margin of the prechoanal foramen (pfc; Fig. 1b, c). The oblique cartilage (cobl) connects the planum terminale to the anterior part of the nasal capsule and forms most of the lateral wall of the nasal capsule (Fig. 1a, b). The infranarial cartilage (inc) projects from the oblique cartilage to form the ventral margin of the naris and bridge the gap between the oblique cartilage and the anterolateral side of the septum nasi (Fig. 1c). The alary cartilage (cal) originates from the anterior portion of the septum nasi and projects laterally to form the dorsal margin of the naris.

A small, globular cartilage lies close to the ventral side of the pila preoptica (Fig. 1a: "palc?") and immediately dorsal to the palatine. It is not connected to the rest of the endocranium and may represent a palatal cartilage (see "Discussion"). At BS 43, the vomer is distinctly crescent shaped. The premaxilla and palatine are elongated posteriorly and flattened horizontally; the lateral margins of both elements are curved downward. The posterior tip of the premaxilla extends to the solum nasi, and the palatine to the level of the pila antotica (Fig. 1c). The occipital arches are almost entirely covered by a perichondral sheet of exoccipital bone (Fig. 1). The perichondral ossification covering the posterior third of the taenia marginalis is the prootic (pro; Fig. 1a, b); this ossification extends slightly onto the otic capsule. The dermal parietal (par) and nasal (nas) roofing bones are plate-like ossifications that are embedded in a large sheet of unmineralized fibrous tissue. The largest element, the parietal, extends from the level of the foramen orbitale to the palatoquadrate (Fig. 1a, b) and is close to the orbital cartilage and taenia marginalis. The smaller nasal lies dorsal to the infranarial cartilage, medial to the oblique cartilage, and lateral to the septum nasi (Fig. 1a, b).

In embryos of BS 47/48 and 48, ossification has increased. Large areas of the posterior endocranium are covered by a sheet of perichondral bone that extends from the otic capsule to the pila antotica (Figs. 2c, d, 3a). A bony lamella projects medially from the dorsomedial surface of the posterior otic capsules (Fig. 2c, e). There are only remnants of the parachordal cartilage, the ventral side of the occipital arch (Figs. 2c, d, 3a), and the orbital and trabecular cartilages. The footplate of the stapes fills nearly the entire fenestra ovalis; it is extensively ossified perichondrally, except in the region of its caudal tip and the most anterior part of the lateral process. The medial process of the stapes is fused to the parachordal cartilage (Figs. 2d, 3f, h). The embryonic palatoquadrate remains cartilaginous dorsally, but otherwise is replaced by a thick layer of perichondral bone that is the quadrate (qu; Fig. 3a, c). The pterygoid process of the quadrate extends slightly anterior to the pila antotica (Fig. 3c, d) and forms a cartilaginous articulation with the parachordal cartilage medially (Fig. 3g). A small, bony process extends anteriorly from the processus pterygoideus and borders the posterior margin of the palatine. The parasphenoid (psph) of embryos in BS 47/48 and 48 is ossified extensively and fills the basicranial fenestra (bcf) of the endocranium (Figs. 2d, 3a, f). In addition, the dermal parasphenoid is fused to parts of the endoskeletal prootic and exoccipital (Fig. 3f), initiating the formation of the os basale (ob). Parts of the oblique cartilage remain cartilaginous (Figs. 2c, d, 3a).

The septum nasi and pila preoptica are covered by a single continuous sheet of perichondral bone. A bony vertical lamella extends backward from the perichondral bone of the posterior part of the septum nasi. This plate of bone is continuous with the pair of lamellae of membrane bone that extend from the perichondral ossifications around the anterior margins of the pilae preopticae; together these elements represent the endoskeletal sphenethmoid (sph; Fig. 2c, d) that forms the anterior wall of the braincase. The dorsal part of the sphenethmoid is a massive triangular ossification between the nasal and frontal (fr) bones (Fig. 2c, e, g). A dermal squamosal (sq) lies lateral to the dorsal portion the quadrate (Fig. 2c, d) and covers parts of the parietal laterally. The squamosal is a uniformly ossified sheet of bone that extends from the quadrate to the posterior edge of the eye, thereby covering the cheek region of the cranium and forming the lateral wall of the adductor chamber and posterior part of the orbit. The squamosal's most anterior margin is dorsolateral to the maxilla (mx) and overlapped by the frontals laterally. The frontal (fr) is the last of the skull-roofing bones to appear (Table 2). It lies between the nasal and the parietal, and is smaller than both of these elements. The three bones distinctly overlap each other forming scarf joints, with the more anterior one always extending over the posterior one for a short distance (Fig. 3a). The overlap between the frontal and the parietal is more extensive than that between the nasal and the frontal. All of the skull-roofing bones are extensively ossified. Medial and lateral to each cartilaginous nasal capsule, the nasal fuses to the premaxilla to form the dermal nasopremaxilla (npm). The premaxillary portion of the nasopremaxilla has increased in size and become crescent shaped; it has a prominent dental

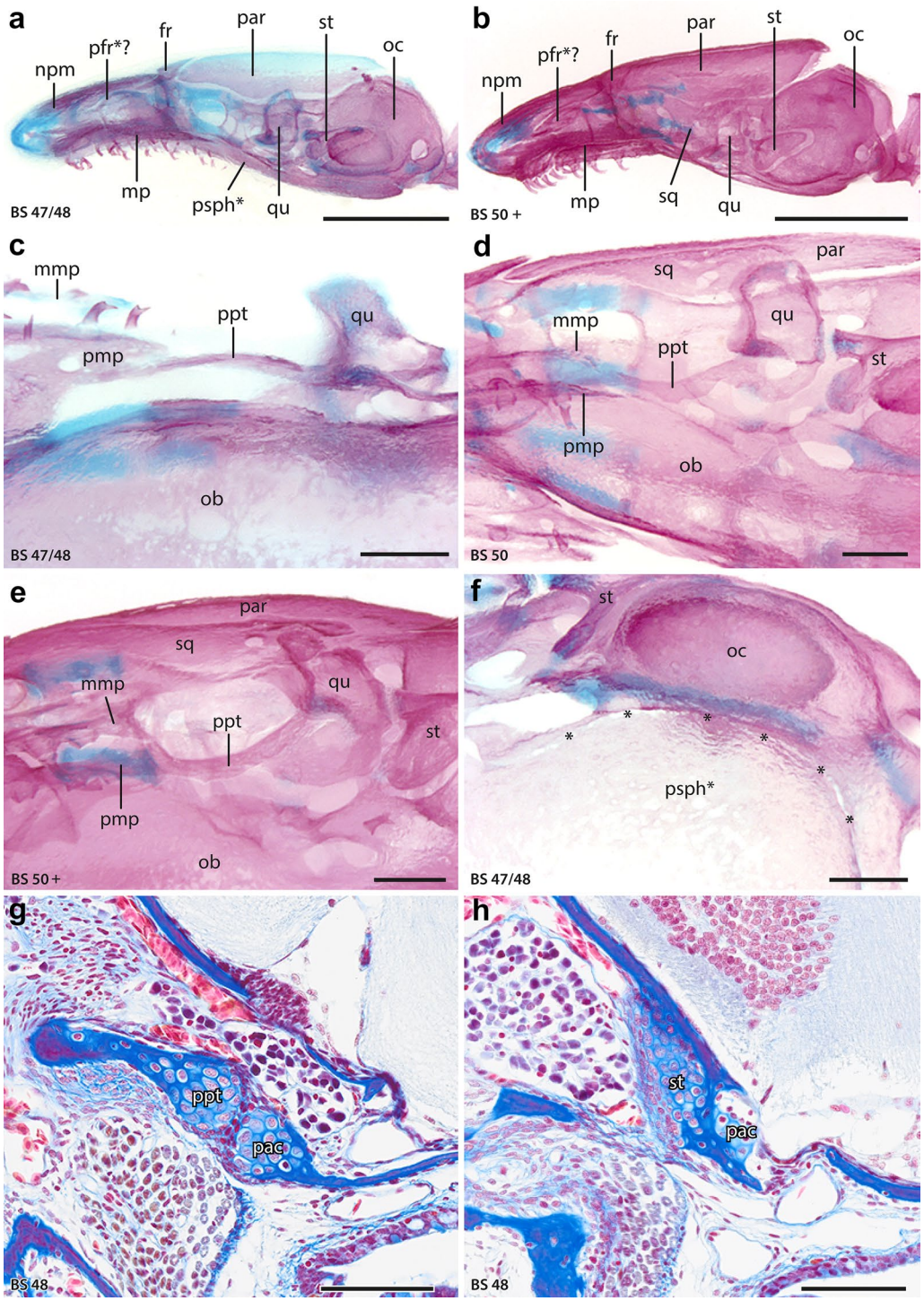

Fig. 3 Aspects of cranial developmental morphology in *Idiocranium russeli*. **a** Skull of Idio6 (BS 47/48) in lateral view. **b** Skull of Idio16 (BS 50+) in lateral view. **c** Quadrate of Idio6 (BS 47/48) in ventral view. **d** Quadrate of Idio11 (BS 50) in ventrolateral view. **e** Quadrate of Idio16 (BS 50+) in ventrolateral view. **f** Posterior skull of Idio16 (BS 50+) in ventral view. **g** Joint between the parachordal cartilage and the processus pterygoideus of the quadrate; transverse section of Idio7 (BS 48) stained with AZAN. **h** Fusion of the stapes and the parachordal cartilage; transverse section of Idio7 (BS 48) stained with AZAN. Asterisk marks points of fusion between the exoskeletal parasphenoid and the endocranium. *fr* frontal, *mmp* maxillar portion of the maxillopalatine, *mp* maxillopalatine, *npm* nasopremaxilla, *ob* os basale, *oc* otic capsule, *pac* parachordal cartilage, *par* parietal, *pfr** prefrontal fused to maxillopalatine, *pmp* palatine portion of the maxillopalatine, *ppt* processus pterygoideus, *psph** parasphenoid fused to endocranium, *qu* quadrate, *sq* squamosal, *st* stapes, *vom* vomer. Scale bars 1 mm in **a, b**; 0.2 mm in **c**–**f**; 0.1 mm in **g, h**

Table 2 Ossification sequence of the skull and lower jaw in *Idiocranium russeli*

Stage	Cranium	Lower jaw
40	[1] vomer	[1] dentary
	[2] exoccipital	[2, 3] mentomeckelian
		[1] coronoid
41	[1] palatine	[1] angular
	[1] premaxilla	
43	[2] prootics	[5] pseudodentary
	[1] parietal	
	[1] nasal	
47/48	[1] frontal	[5] pseudoangular
	[2] stapes	
	[1] parasphenoid	
	[1] nasopremaxilla	
	[1] maxillopalatine	
	[2] quadrate	
	[2, 4] sphenethmoid	
	[1] squamosal	
50	[4, 5] os basale	

Notes on ossification: [1] dermal, [2] perichondral, [3] endochondral, [4] membrane bone, [5] compound bone

lamina bearing some bicuspid teeth. The nasopremaxillae diverge posteriorly, so that the only region in which the pair approach contact is slightly anterior to the sphenethmoid (Fig. 2c, e, g).

The vomer forms the rostral portion of the inner tooth row of the upper jaw. It lies caudal to the nasopremaxilla and bears a distinct dental lamina (Fig. 2d). The anterior processes of the pair of vomers converge slightly and terminate between the paired premaxillary elements (Fig. 2d). The maxilla is present and fused to the dermal palatine to form the maxillopalatine (mp) in embryos of BS 47/48 (Fig. 2d, f, h); the palatine portion of the bone is longer than the maxillary part. The palatine part of the maxillopalatine has a medial postchoanal process that forms the posterior border of the choana (Fig. 2d). The palatine bears a vertical orbital shelf anteromedial to the eye. The maxillopalatine forms the caudal parts of the outer (maxilla portion) and inner (palatine portion) dental arcades of the upper jaw. Some maxillary tooth crowns are developed, but not connected to bone (Fig. 2d). A slender ossification, continuous with the orbital shelf of the palatine via small bony bridges, occurs on the dorsal portion of the maxillopalatine; this structure possesses a foramen for the tentacle canal and may represent a lacrimal or prefrontal bone (Fig. 3a, b; see Discussion). In terms of cranial skeletal development, BS 47/48 and 48 resemble one another and differ mainly in the overall degree of ossification, especially in the more advanced ossification (and fusion) of the elements forming the os basale (prootics, exoccipitals and parasphenoid), as well as the vomer, palatine, and processus pterygoideus in BS 48.

In hatchling and juvenile stages (BS 50/50+), the parachordal cartilage is completely replaced by bone (Fig. 2f, h). The posterior two-thirds of the dermal parasphenoid is completely fused to the endocranium, but fusion marks remain visible along the margin of its anterior third. The dorsomedial projections of bony lamellae of the otic capsules are considerably larger and form the dorsal margin of the foramen magnum (Fig. 2g). The stapes of juveniles completely fills the fenestra ovalis (Fig. 3b). The stapes is nearly fully ossified, save for the cartilaginous connection with the parachordal cartilage. The squamosal has enlarged and extends to the maxillopalatine, fully covering the cheek region laterally (Fig. 3b). The gaps between the skeletal elements of the cranium decrease after hatching, and the skull becomes more solid in construction (Fig. 3a, b). This is best exemplified in older juveniles (BS 50+) by the skull-roofing bones, which are larger and nearly in contact with their antimeres dorsomedially (Fig. 2g). The nasopremaxilla is ossified extensively, especially rostrally. The prefrontal shelf of the maxillopalatine is prominent in BS 50+ juveniles (Fig. 3b). The numbers of teeth in both arcades of the upper jaw increases between hatchling (BS 50) and older (BS 50+) juveniles (Fig. 2f, h). The quadrate is fully ossified in BS 50+, and the broadened anterior lamella of the pterygoid process articulates with the caudal portion of the palatine. The basal articulation between the quadrate and the parachordal cartilage resembles the condition in BS 47/48 and BS 48 embryos. Small parts of the orbital, trabecular, and oblique cartilages remain. The endolymphatic calcium deposits present throughout embryonic development are absent in older juveniles (cf. Figs. 2h, 3a, b). BS 50+ specimens resemble the adults (Fig. 4) and differ only in the extent of the development of the skull-roofing bones and in having a slightly greater degree of cranial flexure (cf. Figs. 3b, 4a).

Lower jaw

At BS 40, Meckel's cartilages (cm) are a bilateral pair of well-chondrified, simple, cylindrical rods, with their anterior tips forming a broad symphysis. The processus condyloideus (pc) articulates with the ventral surface of the palatoquadrate to form the jaw joint. A retroarticular process (prart) is well-developed; it extends well beyond the jaw articulation and projects upward with a slightly elliptical profile. Anterolaterally, the dermal dentary (den) is a flat and transversely arcuate ossification that approximately parallels the anterior tip of Meckel's cartilage. The anterior tip of Meckel's cartilage is ossified peri- and endochondrally to form the mentomeckelian bone (mmk). At this stage, the dentary is

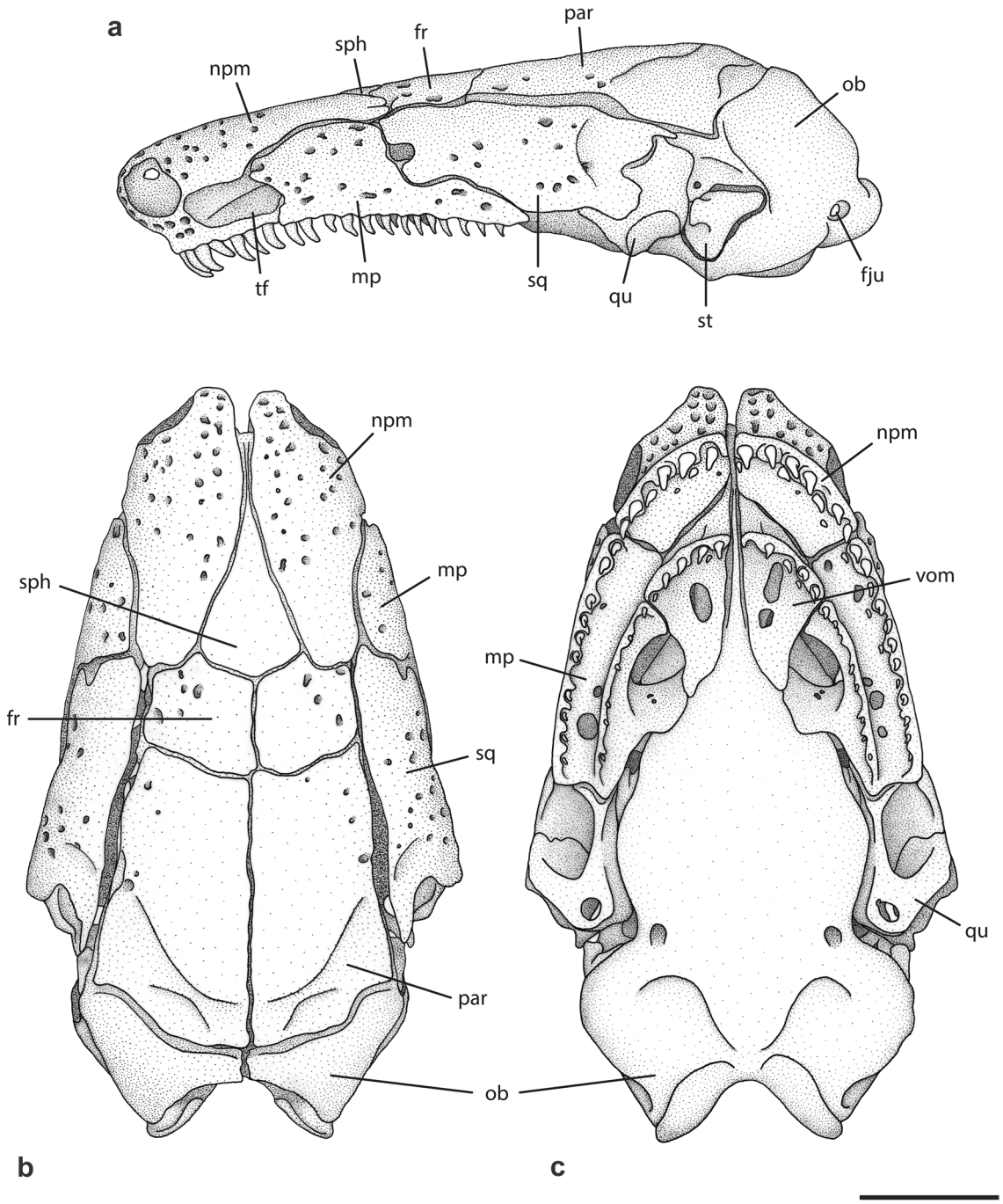

Fig. 4 Adult skull of *Idiocranium russeli* in **a** lateral, **b** dorsal and **c** ventral view. *fju* foramen jugulare, *fr* frontal, *mp* maxillopalatine, *npm* nasopremaxilla, *ob* os basale, *par* parietal, *qu* quadrate, *sph* sphenethmoid, *sq* squamosal, *st* stapes, *tf* tentacular fossa, *vom* vomer. Scale bar 1 mm

contiguous with the mentomeckelian. A dermal coronoid (co) lies posterodorsal to the anterior tip of the cartilage.

The dentary is enlarged in BS 41 embryos, and the coronoid is connected to the perichondral ossifications of Meckel's cartilage via minuscule bony lamellae (Fig. 2a). The dermal angular (ang) lies ventral to Meckel's cartilage; the angular has a rod-like structure and is approximately triangular lateral profile. The anterior tip of the angular is caudal to the dentary and posteriorly, it extends slightly beyond the jaw articulation (Fig. 2a, b). A small, bony lamella extends mediodorsally from the lingual side of the angular but does not seem to represent a separate ossification centre.

At BS 43, ossification of the lower jaw has progressed significantly. The coronoid is slightly curved and is fused extensively to the mentomeckelian. The mentomeckelian bears extensive peri- and endochondral ossifications in the symphyseal region. The dentary is greatly enlarged and covers considerable parts of the labial and dorsal surfaces of Meckel's cartilage (Fig. 1a). Like the coronoid, the dentary is fused extensively to the mentomeckelian in the symphyseal area, thereby initiating the formation of the pseudodentary (psd; Fig. 1a). Mesenchymal tooth anlagen are associated with the dentary and coronoid parts of the pseudodentary. Compared to the angular in BS 41, the bone is longer anteriorly and posteriorly, and covers most of the ventral and lingual surfaces of Meckel's cartilage (Fig. 1a).

In BS 47/48 embryos, the two compound bones forming the lower jaw in adult caecilians are fully developed (Fig. 5a). The articular is represented by a perichondral sheet of bone that covers Meckel's cartilage at the level of the jaw articulation and forms most of the retroarticular process. This endoskeletal element is fused to the dermal angular, forming the pseudoangular (psa). The pseudoangular articulates with the quadrate and bears the processus internus (pi; Fig. 5e, g), which is connected to the bony processus pterygoideus via a ligament. The processus retroarticularis is fully ossified and incorporated in the pseudoangular, but its posterior tip remains cartilaginous until BS 48. Two separate rows of teeth are present; the outer row has many more teeth than the inner (Fig. 5a–e). In both rows, the pedicels of the teeth are fused to their respective bones. The teeth of the outer row usually are larger and associated with the dentary, whereas the teeth of the inner row are smaller and associated with the coronoid. The pseudodentary forms the major part of the labial side of the lower jaw; the pseudoangular comprises most of the lingual side (Fig. 5a–c).

The lower jaw is almost completely ossified in BS 50 and 50 + specimens. Most of Meckel's cartilage is incorporated

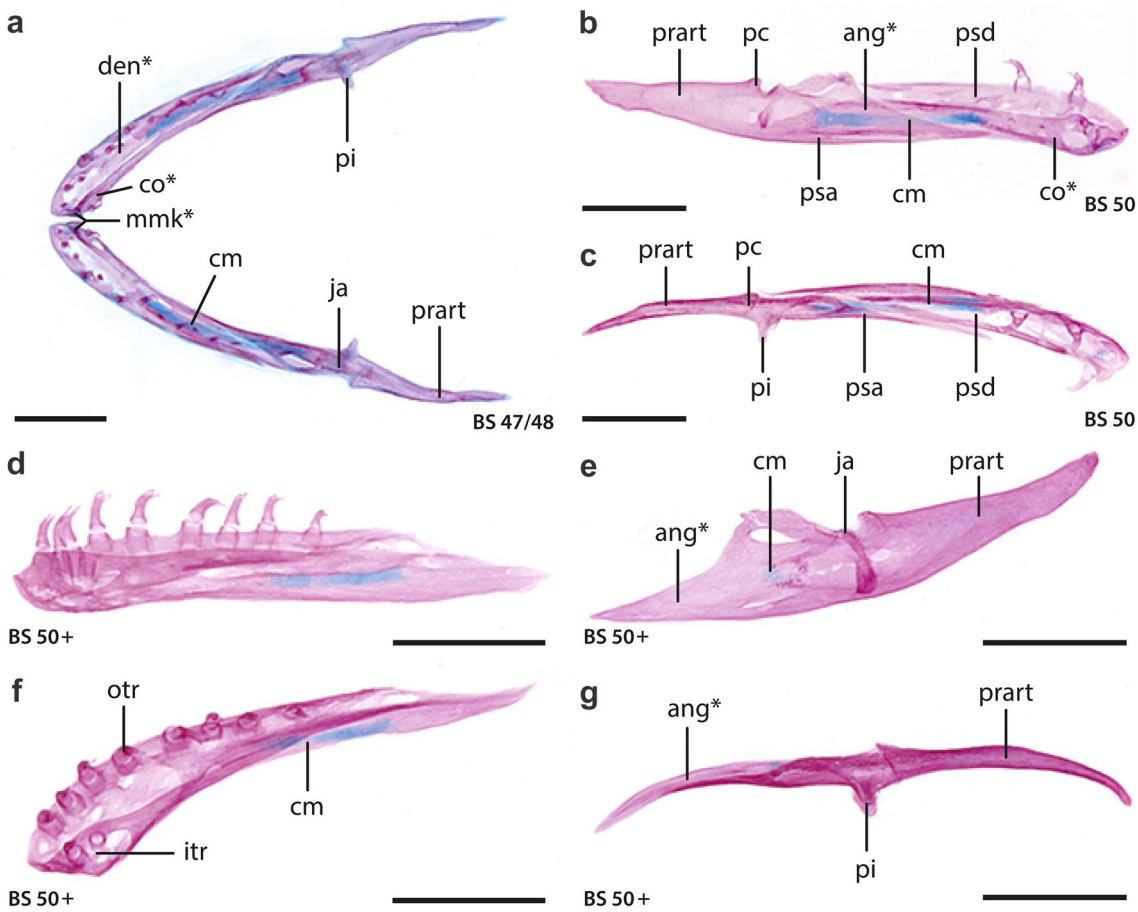

Fig. 5 Developmental morphology of the lower jaw in *Idiocranium russeli*. **a** Dorsal view of the lower jaw of Idio6 (BS 47/48). **b** Medial view and **c** dorsal view of the left mandible of Idio11 (BS 50). **d** Medial and **e** dorsal view of the right pseudodentary of Idio16 (BS 50+). **f** Medial and **g** dorsal view of the right pseudoangular of Idio16 (BS 50+). *ang** fused angular (part of pseudoangular), *cm* cartilago meckeli, *co** fused coronoid (part of pseudodentary), *den** fused dentary (part of pseudodentary), *itr* inner tooth row, *ja* jaw articulation, *mmk** fused mentomeckelian (part of pseudodentary), *otr* outer tooth row, *pc* processus condyloideus, *pi* processus internus, *prart* processus retroarticularis, *psa* pseudoangular, *psd* pseudodentary. Scale bars 0.5 mm

into the pseudodentary and pseudoangular; however, a small portion persists in older juveniles along the posterior part of the pseudodentary (Fig. 5d–g). In these juveniles, tooth development is advanced, with the bicuspid crowns closely associated with their pedicels.

Hyobranchial skeleton

At BS 40, all hyobranchial elements are clearly visible. The posterolateral two-thirds of the ceratohyal is well-chondrified, but the medial third connected to the copula communis is represented only by prechondral condensations. The copula communis (cco) is a weakly chondrified, rod-like structure that connects the ceratohyal (chy) and the ceratobranchials (cb) ventromedially. It is thicker between ceratobranchial I and II than between ceratobranchial II and III. Ceratobranchial I is completely chondrified. Ceratobranchial II is shorter and stouter than ceratobranchial I and their distal tips and medial connection to the copula communis is only weakly chondrified and surrounded by prominent mesenchymal condensations. Ceratobranchial III and IV are not well-chondrified distally. Ceratobranchial IV is small and fused to the mediocaudal edge of ceratobranchial III; this contact is formed mostly by prechondral condensations. The overall shape of the hyobranchial skeleton of BS 41 is similar to that of BS 40 (Fig. 5a), but all elements are fully chondrified and the copula communis is equally developed anterior and posterior to ceratobranchial II (Fig. 6a).

At BS 43, the most anterior part of the copula communis is differentiated into a short basibranchial. The copula communis is absent between ceratobranchial I and II, and only a small mesenchymal projection in front of ceratobranchial II remains (Fig. 6a). A remnant of the copula communis is still present between ceratobranchial II and III. Ceratobranchial III and IV are more extensively fused together.

By BS 47/48, the copula communis is absent and ceratobranchial II and III are fused medially with their antimeres. New cartilage has formed between ceratobranchial III and IV, effectively merging both elements into a single ceratobranchial III/IV (Fig. 6c). At this stage, it is still

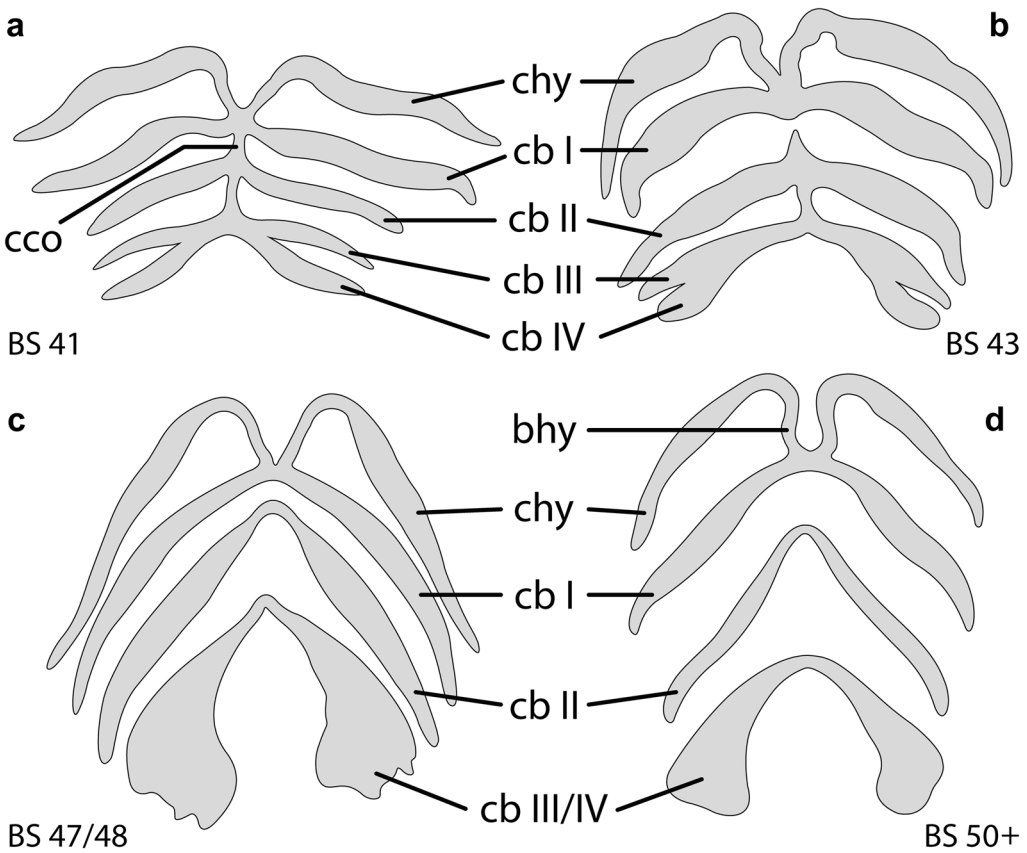

Fig. 6 Development of the hyobranchial skeleton in *Idiocranium russeli*. Drawings of **a, c** and **d** are based on cleared and stained specimens. **b** Based on three-dimensional reconstruction made for Idio5. All panels in ventral view. **a** Hyobranchial skeleton of Idio3 (BS 41). **b** Hyobranchial skeleton of Idio5 (BS 43). **c** Hyobranchial skeleton of Idio6 (BS 47/48). **d** Hyobranchial skeleton of Idio16 (BS 50+). *bhy* basihyale, *cb I* ceratobranchial I, *cb II* ceratobranchial II, *cb III* ceratobranchial III, *cb IV* ceratobranchial IV, *cb III/IV* fused ceratobranchials III and IV, *cco* copula communis, *chy* ceratohyal. Not to scale

possible to identify the outlines of ceratobranchial III and IV and to distinguish both elements from the newly formed cartilage.

The hyobranchial skeleton of juveniles does not differ much from that of BS 47/48 embryos, but all elements appear to be more rounded and robust. Ceratobranchial III and IV are no longer distinguishable from one another, and the fused ceratobranchial III/IV is broadly rounded posterolaterally. The ceratohyal is connected to ceratobranchial I by a U-shaped basihyal (bhy; Fig. 6d).

Axial skeleton

In contrast to the cranial skeletal elements, the axial elements usually form and ossify in a distinct cranial-to-caudal sequence. Axial ossifications are first observed in BS 40 embryos, in which at least the centrum and the neural arches of the atlas and the following three vertebrae have begun to ossify. The rest of the axial skeleton was not sectioned. The centra develop without a cartilaginous precursor as sheath-like, intramembranous ossifications that surround and constrict the notochord. The cartilaginous neural arches ossify perichondrally, from ventral to dorsal, along an anterior–posterior gradient. At BS 41, the centra of 87 vertebrae are apparent in Idio3, and only the most posterior portion of the notochord lacks associated ossifications. Additionally, the first 72 pairs of cartilaginous neural arches are present and associated with their respective centra. The first 39 neural arches are perichondrally ossified. The neural arches of the atlas are entirely covered by a sheet of bone; in contrast, the 39th pair of neural arches is only perichondrally ossified around their ventral bases, where they contact the bony centrum. Approximately, 50 pairs of cartilaginous ribs are present, associated with the first 50 vertebrae following the atlas.

In BS 47/48, centra of 92 vertebrae are present in Idio6. The centra are amphicoelous and spool shaped. Each centrum is associated with a pair of neural arches. All but the last three pairs of neural arches are sheathed in perichondral bone, as are the ribs of the first 20 vertebrae. By the time the juveniles hatch (BS 50), only the last rudimentary pair of neural arches remains cartilaginous. Pre- and postzygapophyses are well-chondrified in all but the last two vertebrae; the ribs of the first 51 vertebrae have perichondral ossifications. In older juveniles (BS 50+), all the ribs have at least a small amount of perichondral ossification, with the posterior ribs being less obviously covered by bone than the anterior ones. The cartilage of the first 10 ribs is completely replaced by bone. The most posterior part of the axial skeleton retains a distinct cartilaginous vestige of the notochord, similar to that described for adult *I. russeli* by Wake (1986).

Musculature

The descriptions of some of the head and anterior trunk musculature are based on specimens in BS 50 and 50+, with notes on the development of individual muscles. Origin and insertion sites of cranial and hyobranchial muscles are summarized in Table 3.

Mandibular musculature

The mandibular musculature innervated by the nervus trigeminus (V) consists of muscles of the adductor group, the m. intermandibularis (mim) and the m. pterygoideus (mpter). The adductor group includes the mm. adductor mandibulae longus, adductor mandibulae internus, adductor mandibulae articularis, and levator quadrati. These muscles are covered laterally by the squamosal and enclosed in the adductor chamber. The m. adductor mandibulae longus is the outermost and largest of the adductor group; it originates on the lateral edge of the parietal and inserts on the dorsal surface of the pseudoangular, slightly in front of the jaw articulation. The m. adductor mandibulae internus is medial to the m. adductor mandibulae longus; it originates from the taenia marginalis part of the os basale and inserts dorsally on the pseudoangular. The m. adductor mandibulae articularis is the smallest adductor muscle; it originates on the rostral part of the quadrate and inserts dorsally on the pseudoangular, caudal to the insertion sites of the other adductors and just anterior to the jaw articulation. A slender m. levator quadrati inserts mediodorsally on the bony processus pterygoideus. This muscle first appears in BS 43 embryos, in which it originates from the ventral side of the taenia marginalis. By BS 48, its origin is on the lateral side of the pila antotica and this configuration remains unchanged in hatchling and juvenile stages. The thin, sheet-like m. intermandibularis is present in the youngest individual examined (BS 40). It originates along the ventromedial side of the pseudoangular from its rostral end to the level of the jaw articulation, and it inserts with its antimere at a midline fascia (Fig. 7a, b). The m. pterygoideus is short and stout and lies along the inner surface of the lower jaw; it originates on the pterygoid process and inserts medially on the retroarcticular process. The m. pterygoideus is ventromedial to the jaw articulation and covered by the m. intermandibularis rostrally, and the m. interhyoideus caudally (Fig. 7).

Hyoid musculature

The hyoid musculature consists of all muscles innervated by the nervus facialis (VII) and associated with the hyoid arch; included are the depressor group and the m. interhyoideus posterior. There is no trace of m. hyomandibularis in any of the specimens examined. The depressor group comprises the

Table 3 Cranial muscles of *Idiocranium russeli* investigated in the present study, including points of origin and insertion, as well as innervation

Nerve	Muscle	Origin	Insertion
[V]	m. adductor mandibulae articularis	rostral quadrate	pseudoangular (dorsal)
[V]	m. adductor mandibulae internus	taenia marginalis	pseudoangular (dorsal)
[V]	m. adductor mandibulae longus	parietal (lateral)	pseudoangular (dorsal)
[IX/X]	m. cephalodorsosubpharyngeus	dorsal fascia of epaxial musculature	ceratobranchial III/IV (and lateral wall of pharynx)
[VII]	m. depressor mandibulae	squamosal and parietal	processus retroarticularis (dorsal)
[VII]	m. depressor mandibulae posterior	dorsal fascia of epaxial musculature and parietal	processus retroarticularis (medial)
[XII]	m. genioglossus	rostral pseudodentary (lingual)	tongue epithelium
[XII]	m. geniohyoideus	fascia of m. rectus cervicis	lower jaw (lingual)
[VII]	m. interhyoideus posterior	ventromedian raphe	processus retroarticularis (ventral)
[V]	m. intermandibularis	pseudoangular (medial)	median raphe
[V]	m. levator quadrati	pila antotica (lateral)	processus pterygoideus (dorsomedial)
[S]	m. obliquus externus superficialis	fascia dorsalis	fascia of hypaxial musculature
[S]	m. obliquus externus profundus pars nuchalis	ventrolateral fascia of hypaxial musculature	rib of second vertebra (laterodistal)
[V]	m. pterygoideus	processus pterygoideus	processus retroarticularis (medial)
[XII]	m. rectus cervicis	fascia of m. rectus. abdominis	ceratobranchial I
[IX/X]	m. subarcualis rectus I	ceratobranchial I	ceratohyal
[IX/X]	m. subarcualis rectus II–IV	ceratobranchial III/IV	ceratobranchial I
[IX/X]	m. subarcualis obliquus II	ceratobranchial II	ceratobranchial I
[IX/X]	m. subarcualis obliquus III	ceratobranchial III/IV	ceratobranchial II

Innervation: [V] n. trigeminus, [VII] n. facialis, [IX] n. glossopharyngeus, [X] n. vagus, [XII] n. hypoglossus, [S] spinal nerve

m. depressor mandibulae (mdm) and the m. depressor mandibulae posterior; together these muscles function to open the jaw and are antagonists of the adductor muscles (Nussbaum 1983). The m. depressor mandibulae is massive and originates on the laterocaudal surface of the squamosal and the dorsocaudal surface of the parietal. Additionally, some of its caudal fibres are connected to the dorsal trunk musculature via a fascia. The m. depressor mandibulae (mdm) inserts dorsally on the retroarticular process (Fig. 7a, c). The fibres of this muscle are present in BS 43 embryos and already attached to their insertion site. The m. depressor mandibulae posterior is short and thin, and lies medial to the posterior part of the m. depressor mandibulae. The two depressors are partially fused. The m. depressor mandibulae posterior can be identified by its oblique fibre orientation and a medial insertion on the retroarticular process. It first appears in BS 48 embryos, in which it originates from the dorsal trunk musculature via a fascia. Additionally, some of its fibres originate from the posterior parietal bone, in hatching and juvenile stages. The m. interhyoideus posterior is a large, superficial, fan-shaped muscle. It originates from the ventral side of the retroarticular process and extends broadly over part of the ventrolateral trunk musculature, where it inserts via a fascia. Posteriorly, it reaches the sixth myomere and covers parts of the m. geniohyoideus (mgh) and the m. rectus cervicis (mrc; Fig. 7a, b). In older juveniles (BS 50+), most of the rostral fibres of the paired m. interhyoideus posterior are in contact with one another anteromedially, immediately caudal to the m. intermandibularis. The anterior fibres of the m. interhyoideus posterior have a general ventromedial orientation, but posteriorly, the fibre orientation is more posteroventral or directly posterior.

Hyobranchial musculature

This includes the mm. subarcuales recti and the mm. subarcuales obliqui, as well as the m. cephalodorsosubpharyngeus (mm. levatores arcuum branchialium (I–IV) of Kleinteich 2009). The hyobranchial muscles are innervated by the nervus glossopharyngeus [IX] and nervus vagus [X]. The mm. subarcuales recti and the mm. subarcuales obliqui are the ventral hyobranchial muscles. The former extend laterally between the ceratobranchials, whereas the latter are situated medioventrally between them. The following individual muscles could be identified: m. subarcualis rectus I, m. subarcualis rectus II–IV, and mm. subarcuales obliqui II and III. The m. subarcualis rectus I originates on the ventral surface of the lateral ceratobranchial I; its fibres are anteroventrally oriented and it inserts posterolaterally on the ceratohyal. The m. subarcualis rectus II–IV originates on the anterolateral surface of the ceratobranchial III/IV and it inserts posteriorly on the lateral ceratobranchial I. The m. subarcualis rectus II–IV extends ventrally to the mm. subarcuales obliqui. The m. subarcualis obliquus II originates on the anterolateral

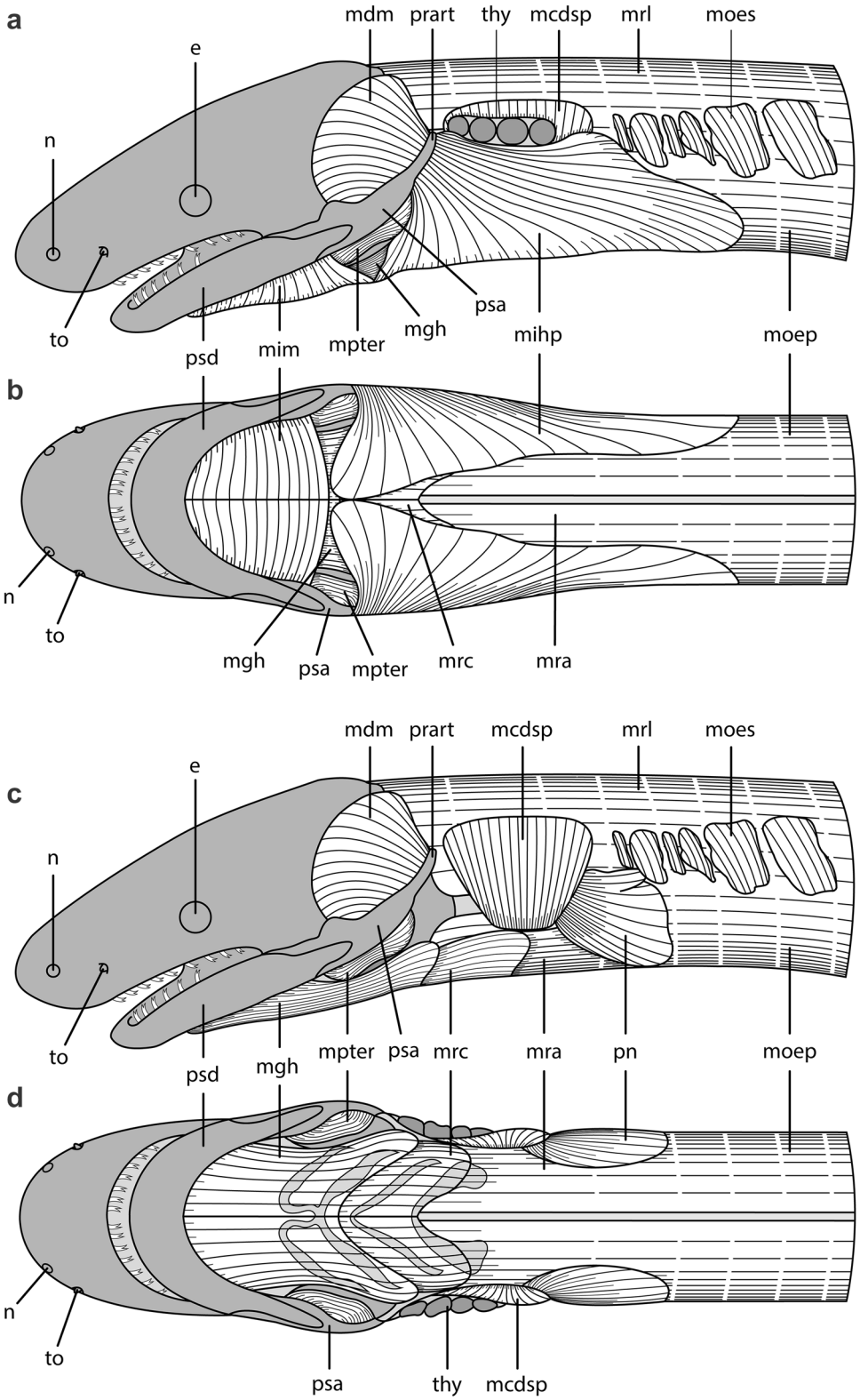

Fig. 7 Juvenile musculature of *Idiocranium russeli*. **a** Lateral and **b** ventral view of superficial musculature of Idio16 (BS 50+). **c** Lateral and **d** ventral view of the musculature after removal of the m. interhyoideus posterior and the m. intermandibularis; thymus gland removed in **c**. Shape and position of the hyobranchial skeleton is indicated in **d**. Superficial anterior trunk musculature simplified. *e* eye, *mcdsp* m. cephalodorsosubpharyngeus, *mdm* m. depressor mandibulae, *mgh* m. geniohyoideus, *mihp* m. interhyoideus posterior, *mim* m. intermandibularis, *moep* m. obliquus externus profundus, *moes* m. obliquus externus superficialis, *mpter* m. pterygoideus, *mra* m. rectus abdominis, *mrc* m. rectus cervicis, *mrl* m. rectus lateralis, *n* nostril, *pn pars nuchalis* of the m. obliquus externus profundus, *psa* pseudoangular, *psd* pseudodentary, *prart* processus retroarticularis, *thy* thymus gland, *to* tentacle organ. Not to scale

surface of ceratobranchial II and it inserts ventromedially on ceratobranchial I. The m. subarcualis obliquus III originates on the anterolateral surface of ceratobranchial III/IV and inserts on the ventromedial margin of ceratobranchial II. The fibres of the mm. subarcuales obliqui curve from laterodistal to ventromedial. The m. cephalodorsosubpharyngeus (mcdsp) is distinct and approximately trapezoidal, with fibres oriented primarily dorsoventrally. It originates

from the dorsal trunk musculature of the first three trunk myomeres via a dorsal fascia and inserts on ceratobranchial III/IV (Fig. 7c, d) via a tendon. Additionally, some of its fibres are attached to the lateral wall of the pharynx in BS 43 and BS 48 embryos. The first loose fibres of this muscle appear in BS 40. Most of the m. cephalodorsosubpharyngeus is covered laterally by the m. interhyoideus posterior and the thymus gland (thy; Fig. 7a). Separate mm. levatores arcuum branchialium I–IV could not be identified in any of the specimens examined.

N. hypoglossus [XII]–innervated musculature

This comprises the tongue muscles—the m. genioglossus and m. geniohyoideus (mgh), and the m. rectus cervicis (mrc). The m. genioglossus forms the muscular portion of the tongue. It is a loose bundle of fibres that originate on the lingual surface of the rostral part of the pseudodentary. The fibres fan out mediodorsally within the tongue and terminate beneath the dorsal tongue epithelium (Fig. 8b). The first fibres differentiate early during development (BS 43; Fig. 8a). The m. geniohyoideus lies ventral to the m. genioglossus, approximately parallel to the longitudinal body axis. The m. geniohyoideus originates from the anteroventral part of the m. rectus cervicis via a fascia at a level between the ceratobranchials I and II, and inserts on the lingual surface of the lower jaw (Fig. 6c, d). The m. rectus cervicis originates from the m. rectus abdominis (mra) via an anteroventral fascia at the level of ceratobranchial III/IV (Fig. 7c, d). The muscle fibres run from posterior to anterior and insert on the caudal surface of the medial part of ceratobranchial I. Some of the more medial fibres extend farther anterior and attach to the basihyal.

Anterior somatic musculature

The trunk musculature is innervated by the segmental spinal nerves. It is separated into the epaxial and hypaxial musculature (dorsal and ventral to the horizontal septum, respectively). The epaxial musculature mainly comprises the m. dorsalis trunci, m. rectus lateralis (mrl), and the deeper muscles connected to the vertebrae. The hypaxial musculature comprises the m. obliquus externus superficialis (moes), m. obliquus externus profundus (moep), m. rectus abdominis, m. obliquus internus and m. transversus (Nussbaum and Naylor 1982). Laterally, a segmental m. obliquus externus superficialis forms a row of nearly rectangular muscle sheets. It is the most superficial muscle of the body wall, and its fibres are oriented dorsoventrally, with a slight posterior inclination towards the ventral pole (Fig. 7a, c). The m. rectus lateralis is elongated and dorsal (Fig. 7a, c). Anteriorly, it is associated with the posterior side of the skull. The sheet-like m. obliquus externus

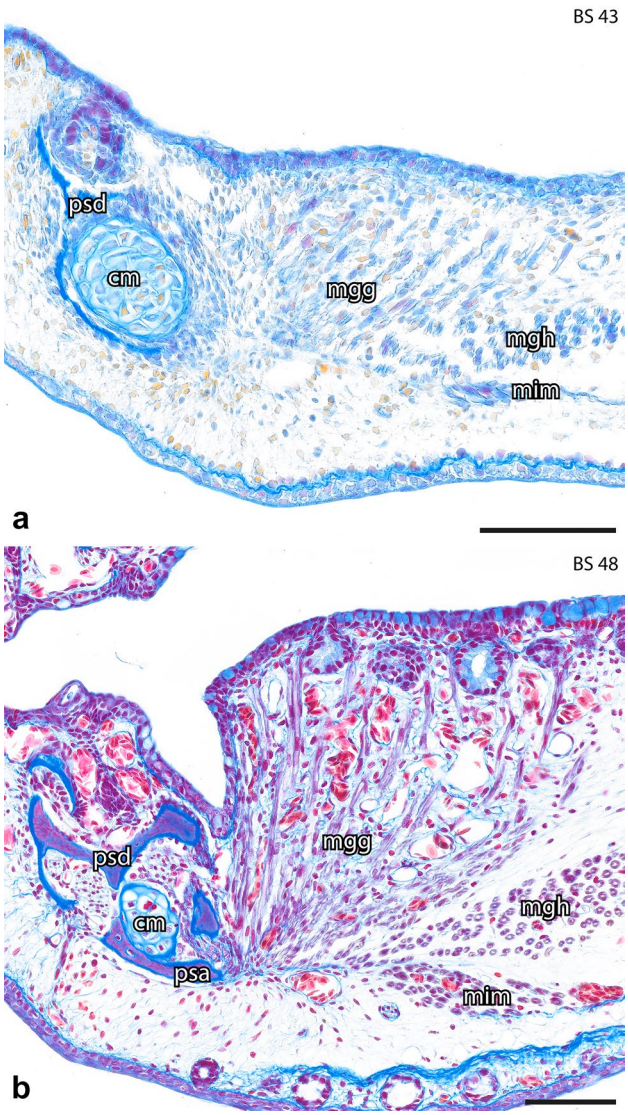

Fig. 8 Development of the genioglossus muscle in *Idiocranium russeli*. Transverse section through the right side of the lower jaw in **a** BS 43 (Idio5) and **b** BS 48 (Idio7). *cm* cartilago meckeli, *mgg* m. genioglossus, *mgh* m. geniohyoideus, *mim* m. intermandibularis, *psa* pseudoangular, *psd* pseudodentary. Scale bars 100 µm

profundus forms the superficial ventral portion of the muscular body wall (Fig. 7). It is associated with the m. rectus abdominis, which lies medioventral to it. Additionally, embryonic and juvenile *I. russeli* possess a muscle that inserts at the distal tip of the first pair of ribs and originates on the ventrolateral trunk musculature of the fourth myomere. This muscle is anteroventral to the m. obliquus externus superficialis and has been described previously for caecilian amphibians (Wilkinson and Nussbaum 1997) in which it was termed the pars nuchalis (pn) of the m. obliquus externus profundus (Fig. 7c, d). The first fibres of this muscle were observed in BS 43 embryos.

Discussion

Chondrocranium

The structure of the chondrocranium is quite homogenous in caecilians (Duellman and Trueb 1986; Wake and Hanken 1982; Müller 2006), and the chondrocranium of *I. russeli* is not unusual. There is a foramen palatinum in the parachordals; this has only been reported for *H. rostratus, G. alternans*, and *Epicrionops petersi* (Müller 2006). The ventromedial process of the stapes is closely associated with the parachordal cartilage. In BS 43 *I. russeli*, the space between stapes and parachordal is filled with mesenchymal cells, and by BS 47/48 the two cartilages appear to be fused (Fig. 3f, h). This condition also occurs in embryos of *H. rostratus* (Müller 2006), but not in embryos of *G. ramaswamii* (Müller et al. 2005). The narrow solum nasi seen in BS 43 *I. russeli* also occurs in *H. rostratus*, but not in *G. ramaswamii* (Müller 2006; Müller et al. 2005). The general morphology and development of the nasal capsules of *I. russeli* closely resembles those of other indotyphlids and that of the dermophiid *Dermophis mexicanus* (Wake and Hanken 1982). At BS 43, an isolated, small, globular cartilage lies ventral to the pila preoptica and dorsal to the palatine ossification. A similar element has been described as a palatine cartilage in embryos and larvae of species of the ichthyophiid *Ichthyophis* (Peter 1898; Visser 1963), but this cartilage is more posterior in position than in *I. russeli*. At a comparable position to the globular cartilage in *I. russeli*, there is a cartilaginous "postchoanal commissure" in foetuses of the viviparous scolecomorphid *Scolecomorphus kirkii* (Müller et al. 2009). However, the postchoanal commissure is a continuous part of the chondrocranium in *S. kirkii;* thus, it seems an unlikely homologue to the cartilage in *I. russeli*, which we tentatively interpret as a palatine cartilage comparable to that in *Ichthyophis*.

Ossifications

The overall composition and development of cranial and mandibular ossifications in *I. russeli* resemble those of other caecilians examined thus far; see Wake (2003) and Müller (2006) for detailed revisions of cranial osteology of some caecilians. However, given the extensive endocranial ossification and the tendency for individual bones to fuse to form compound elements in caecilians, the exact composition and homology of some of the elements remains unclear (Müller 2006). This is the case in the two main components of the adult neurocranium, i.e., the os basale and the sphenethmoid. The compound os basale is the largest element of the adult caecilian skull. Originally, it was described as being composed of up to eight individual ossifications (Marcus et al. 1935), but more recent studies failed to confirm several of these (e.g., Wake and Hanken 1982; Müller 2006). In *I. russeli*, we identified only three centres of ossification for the os basale—the parasphenoid, prootics, and exoccipitals. Three centres also occur in *H. rostratus* (Müller 2006), *G. ramaswamii* (Müller et al. 2005), and *D. mexicanus* (Wake and Hanken 1982), with the "taenia marginalis ossification" of the latter species likely corresponding to the prootics of the indotyphlids. The perichondral ossifications of the parachordal and ventral otic capsule, which were described as a separate basisphenoid in *G. ramaswamii* and *D. mexicanus*, are contiguous with the exoccipitals and a separate basisphenoid is absent. The sphenethmoid is the most complex structure of the caecilian cranium, and the number and homology of its constituent parts are unclear (Wake and Hanken 1982; Müller 2006). This is largely a result of its late, but rapid formation after the formation of most of the surrounding dermal bones. Unfortunately, our material of *I. russeli* has a crucial gap; no sphenethmoid is present at BS 43, and the element is nearly fully formed in the next available stage (47/48); this precludes any insights into its formation. *Idiocranium russeli* is the only caecilian species in which the dorsal part of the sphenethmoid forms a large, characteristically triangular part of the skull roof (Parker 1936; Taylor 1969; Wake 1986). The unusual shape of the sphenethmoid in *I. russeli* is established by BS 47/48 and the greatly enlarged, triangular dorsal part is clearly visible (Figs. 2c, 4b). The nasal is unusually long and extends farther posteriorly than in other caecilians, but the frontal is exceptionally short (Taylor 1969; Wake 2003).

There is a bony septomaxilla and/or a prefrontal element in adult rhinatrematids, ichthyophiids, and scolecomorphids. These elements also occur in embryos of the dermophiid *D. mexicanus*, in which the septomaxilla is incorporated into the nasopremaxilla and the prefrontal into the maxillopalatine (Wake and Hanken 1982). We did not find a septomaxilla in any stage of development in *I. russeli*. A septomaxilla is also absent in the Indo-Seychelles indotyphlids *H. rostratus* and *G. ramaswamii*, but both of the latter have another ossification anterior to the eye and dorsal to the maxilla and palatine (Müller et al. 2005; Müller 2006); embryos of *I. russeli* also have a distinct bony element in the same position. In *I. russeli*, the bone is connected to the orbital shelf of the maxillopalatine via small bony bridges (BS 47/48), and it has a foramen through which the tentacular canal passes. Its close association with the tentacular canal, a homologue of the ductus nasolacrimalis of other tetrapods (Billo and Wake 1987), led Müller et al. (2005) to consider it a homologue of the lacrimal bone in *G. ramaswamii*. However, it is

unclear whether this element is a separate bone in *I. russeli* or instead an extension of the orbital shelf of the maxillopalatine, because the connection between them is already established in BS 47/48 embryos. The correct homology of this so-called lacrimal in caecilians is equivocal (Müller et al. 2005). In adult ichthyophiids and scolecomorphids, a separate element in a comparable, although a somewhat more lateral position, usually has been considered to be a prefrontal (Wake 2003). Wake and Hanken (1982) described a prefrontal that fuses with the maxillopalatine during the development of *D. mexicanus*, and this element may be homologous with the lacrimal described for *G. ramaswamii* and *H. rostratus*. Unfortunately, no detailed information is available for the development of the maxillopalatine in Ichthyophidae or Scolecomorphidae, and it is unknown whether two (lacrimal and prefrontal) or only a single ossification is present in the immediate preorbital area in these taxa.

Nine separate centres of lower jaw ossification were described by Eifertinger (1933) and Marcus (1933) for *H. rostratus* (but see Müller 2006). We found only five in *I. russeli*—the dentary, coronoid, mentomeckelian, angular, and articular. A prearticular is absent in embryos of *I. russeli, H. rostratus* (Müller 2006), and *D. mexicanus* (Wake and Hanken 1982), but present in *G. ramaswamii* (Müller et al. 2005). A complementary, present in *D. mexicanus*, is absent in all species of indotyphlids that have been examined. A tooth-bearing coronoid is present in *I. russeli* in a comparable position to the coronoid of *G. ramaswamii* and *H. rostratus*, and the "splenial" described for *D. mexicanus*. In addition to the "splenial", Wake and Hanken (1982) also described a "coronoid" for *D. mexicanus*. It is unclear whether that "coronoid" is tooth-bearing, but the bone may be an additional element of the coronoid series. In indotyphlids, only one coronoid seems to be present [see Müller et al. (2005) for a more detailed discussion of lower jaw elements]. In *I. russeli* a small, bony process that points medially, the processus internus, is present immediately anterior to the jaw articulation, as is characteristic for caecilians in general (Wake 2003). We found a ligament connecting the ventral surface of the processus pterygoideus (posterior to the attachment site of the m. pterygoideus) with the processus internus of the pseudoangular. This ligament is also present in prehatching and juvenile stages of *G. ramaswamii* and *H. rostratus* (Theska, pers. obs.) and might play a role in storing elastic energy during jaw opening and closing.

Embryos and hatchlings of *I. russeli* lack a specialized, deciduous dentition. Instead, from the earliest inception, *I. russeli* teeth have the typical adult morphology, which provides additional corroborative evidence that maternal dermatophagy is absent in Indotyphlidae (San Mauro et al. 2014).

Ossification sequence

The ossification sequence of *I. russeli* (Table 2) resembles those of *G. ramaswamii* and *H. rostratus* (Müller et al. 2005; Müller 2006), but owing to the gap in sampling between BS 43 and 47/48, this assessment must be considered preliminary. The early formation of the coronoid and late formation of the frontal in embryos of *I. russeli* are obvious differences relative to the sequences of other species (Wake and Hanken 1982; Müller et al. 2005; Müller 2006). Comparing the available ossification sequences, the three direct-developing indotyphlids—*I. russeli, H. rostratus*, and *G. ramaswamii*—are more similar to each other than each is to the viviparous *D. mexicanus*. Early development is highly correlated with reproductive mode in amphibians (e.g., Hanken 2003; Schweiger et al. 2017). Foetuses of the viviparous *D. mexicanus* apparently feed on the hypertrophied lining of the maternal oviduct; thus, earlier ossification of the elements associated with the jaw articulation and suspension in this species (Wake and Hanken 1982; Müller 2006) may reflect differences in life history apart from phylogenetic history (cf. Pérez et al. 2009).

Hyobranchial skeleton

Overall, the ontogeny of the hyobranchial skeleton of *I. russeli* is remarkably similar to that of *G. ramaswamii* and, to a slightly lesser degree, that of *D. mexicanus* (Wake and Hanken 1982; Wake 2003; Müller et al. 2005). The shapes of the pharyngeal arches of both indotyphlids are nearly identical; however, development seems to proceed faster in *I. russeli*. In BS 41 embryos of *I. russeli*, chondrification of the hyobranchial elements is more advanced than in embryos of *G. ramaswamii* of the same stage, and the reduction of the copula communis between ceratobranchial I and II in BS 43 embryos of *I. russeli* is as pronounced as in BS 45 embryos of *G. ramaswamii* (Müller et al. 2005). The shape and early fusion of ceratobranchial III and IV are similar in *I. russeli, G. ramaswamii*, and *D. mexicanus*. In contrast, ceratobranchial IV is prominent in *H. rostratus* and only fuses to ceratobranchial III late in development (Müller 2006). In *H. rostratus*, ceratobranchial III and IV also possess elongated and curved distal ends that are associated with the gill slit, which persists until late in the development in this species (Müller, pers. obs.). There are further differences between the shape of the basihyal in *H. rostratus* and that in *I. russeli, G. ramaswamii*, and *D. mexicanus* (see Müller 2006).

Musculature

The configuration of the juvenile musculature of *I. russeli* resembles that of adults as described by Wake (1986) with some notable exceptions. Wake (1986) reported separate

anterior and dorsal portions of the m. depressor mandibulae, but in all specimens investigated here, the m. depressor mandibulae is a massive, fan-shaped muscle without externally visible subdivisions (Fig. 7a, c). We did, however, observe a much smaller and slender m. depressor mandibulae posterior, posteromedial to the m. depressor mandibulae; possibly, these two muscles are equivalent to the bicapitate m. depressor mandibular described by Wake (1986). Wake (1986) also described the m. intermandibularis as being (uniquely, among caecilians) distinctly segmented and comprised of several distinct muscle bundles. We did not observe this phenotype and all specimens that we examined had a single, extensive and continuous m. intermandibularis typical of all other caecilians investigated so far (e.g. Kleinteich and Haas 2007; Wilkinson and Nussbaum 1997). Additional adult *I. russeli* should be investigated to reassess the highly unusual adult form of this muscle reported by Wake (1986).

Idiocranium russeli possesses a fourth mandibular adductor, the m. levator quadrati. This muscle has no known homologues in batrachian amphibians (Kleinteich and Haas 2007). Functionally, it may restrict the degree of downward rotation of the quadrate during phases of contraction of the other three adductors (Duellman and Trueb 1986; Kleinteich and Haas 2007). Muscles exclusive to larvae, such as the m. hyomandibularis (Kleinteich 2009), are absent in embryonic and juvenile *I. russeli;* likewise, they also are absent in *G. ramaswamii* (Kleinteich 2009), the only other indotyphlid caecilian for which data are available. Kleinteich (2009) described the small m. depressor mandibulae posterior to be attached to the ceratohyal in larvae of biphasic caecilians, and to shift its insertion to the retroarticular process during metamorphosis. In embryonic *G. ramaswamii*, some fibres of this muscle are attached to the ceratohyal, but these are reduced or remodelled in juveniles (Kleinteich 2009). Such an insertion on the ceratohyal is absent in any observed stage of development in *I. russeli*. Kleinteich (2009) postulated homology of the m. cephalodorsosubpharyngeus with the levator muscles of the pharyngeal arches. This was based on the observation that the m. cephalodorsosubpharyngeus has separate heads in *D. mexicanus;* the most anterior head is attached to ceratobranchial I in early ontogeny, whereas the others insert on the wall of the pharynx and lack contact with the hyobranchial skeleton. We found the precise attachment site of the m. cephalodorsosubpharyngeus in *I. russeli* difficult to identify, with only some fibres being attached to the lateral wall of the pharynx in embryonic stages (BS 43 and 48). However, most of this muscle in *I. russeli* inserts on ceratobranchial III and IV in BS 43 embryos, and on the fused ceratobranchial III/IV via a tendon in BS 48 embryos and hatchlings/juveniles. This observation lends support to the levator homology hypothesis proposed by Kleinteich (2009).

The configuration of the ventral hyobranchial muscles of *I. russeli* largely corresponds to that of larval *Ichthyophis* (Kleinteich and Haas 2011). These muscles are not exclusively larval features and are mostly maintained in adults (Kleinteich 2009). Interestingly, the m. subarcualis rectus II–IV, which inserts on ceratobranchial II in *Ichthyophis kohtaoensis* (Kleinteich and Haas 2011), is attached to ceratobranchial I in *I. russeli* and *H. rostratus* (Kleinteich 2009).

Miniaturization in *Idiocranium russeli*

Idiocranium russeli is among the smallest species of caecilians (Gower et al. 2015; Maddock et al. 2018) and has a number of morphological peculiarities (Parker 1936; Wake 1986) that have been interpreted to have resulted from miniaturization (Wake 1986). The most notable of these are cranial skeletal features, including the reduction in the sizes of the frontal and vomer, the large gap between the nasals and the frontals that exposes the sphenethmoid, disproportionately large nasal cupulae (anterior, extra-cranially visible part of the nasal capsule) and otic capsules, an extensively ossified sphenethmoid, an absence or reduction of suturing or overlap among several dermal elements, a reduced degree of ossification of the terminal vertebrae and ribs, and the presence of a cartilaginous terminal notochord (Wake 1986). In the absence of relevant ontogenetic data, Wake (1986) inferred that the putatively miniaturized features of adult *I. russeli* might have resulted from the heterochronic process of progenesis (sensu Alberch et al. 1979). With our developmental data, we can test this hypothesis.

A number of morphological features of *I. russeli* seem to be the result of hypomorphosis (sensu Reilly et al. 1997; progenesis of Alberch et al. 1979), which results from an early offset of a developmental signal. Hypomorphosis seems to best explain the reduced degree of suturing and midline contact between the nasal, frontal, parietal, vomer, and others (Fig. 4), along with the retention of a notochord and the reduced ossification of the terminal axial skeletal elements. Wake (1986) also noted the small sizes of the vomer and frontal. The smaller sizes of the vomer and nasal seem to reflect a lack of growth toward the midline, and are consistent with hypomorphosis. The frontal, however, appears late in the ontogeny of *I. russeli;* its onset of ossification seems to have shifted relative to the onset of this bone in *G. ramaswamii* and *H. rostratus*. Therefore, the small adult frontal may be the result of both post-displacement (a later onset of the ossification signal) and hypomorphosis (an earlier offset of the ossification signal; Reilly et al. 1997).

The nasal cupula seems relatively large in adult *I. russeli*, as is the bony narial aperture in the nasopremaxilla through which the nasal cupula projects. The increased size of the bony narial aperture likely resulted from a decreased degree of ossification, which would be consistent with

hypomorphosis. Thus, it seems as though the nasal cupula is not larger, but rather more of it is externally visible. However, the adult otic capsule does not seem to be substantially enlarged relative to those of various different species (Wake 2003). We measured selected specimens of *H. rostratus* illustrated by Müller (2006) and compared these with *I. russeli*. In a BS 47 embryo of *H. rostratus*, the relative length of the otic capsule is 23.7% of skull length compared to 20.6% in a BS 47/48 embryo of *I. russeli*, and these proportions do not change in older specimens. Therefore, it seems that *I. russeli* does not actually have proportionately larger nasal cupulae and otic capsules. Although inferring heterochronic processes from adult morphology can be misleading (Hanken and Wake 1993), most of Wake's (1986) suggestions regarding osteology are confirmed or refined by our ontogenetic data.

Direct development in *Idiocranium russeli* and the re-evolution of larvae in Indotyphlidae

Direct development—the loss of a free-living larva combined with hatching at a postmetamorphic stage—does not simply lead to a shift in hatching time (i.e., to an incorporation of the larval phase into embryonic development). Instead, it involves comprehensive ontogenetic repatterning that leads to a large-scale reduction or complete loss of most larval-specific traits and an early appearance of an adult-like morphology (Hanken 2003). Based on the description of the egg clutches found by Sanderson (1937) and the absence of larval features in the smallest (51 mm total length) available specimen of the type series (Parker 1936), *I. russeli* has been assumed or inferred to be direct developing (Wake 1977; San Mauro et al. 2014). In addition, Gower et al. (2015) made a preliminary examination of encapsulated embryos and hatchlings as small as ca. 35 mm total length and found no indications of larval characters. This is confirmed by our detailed observations reported here. Typical external larval features (Dünker et al. 2000; San Mauro et al. 2014) are either absent (gill slits, lateral line organs, tail fin) or greatly reduced (labial folds) in embryonic *I. russeli*. At the same time, characters such as the tentacle anlage, which starts to develop in larvae in biphasic species, are present in the youngest embryos of *I. russeli* examined (BS 40) and seem to be fully differentiated by BS 47/48, well before hatching. A similar pattern is seen in the skeletal and muscular development. The fusion of the maxilla and palatine, and of the premaxilla and nasal occurs during metamorphosis in most biphasic species (Müller 2007), but it is completed well before hatching in *I. russeli*. The squamosal of *I. russeli* seems to rapidly cover the cheek region and has more or less the same extent as in the adult by BS 47/48. Ceratobranchial IV, which remains a separate element until metamorphosis in biphasic species, fuses to ceratobranchial III early during development, and the adult configuration of the hyobranchial skeleton is established well before hatching. Exclusively larval muscles such as the m. hyomandibularis, m. interhyoideus and separate mm. levatores arcuum branchialium (I–IV) are absent, whereas adult muscles such as the m. genioglossus and m. cephalodorsosubpharyngeus appear early in embryonic development. The lack of an attachment site of the m. depressor mandibulae posterior on the ceratohyal also seems to be a derived trait within the context of the evolution of direct development (Kleinteich 2009).

Our observations reveal that *I. russeli* has few larval traits and that its development is characterized by features indicative of profound ontogenetic repatterning. In this regard, *I. russeli* resembles the Indian indotyphlid *G. ramaswamii* more closely than it does the Seychelles *H. rostratus*. Although a direct developer, *H. rostratus* has a number of traits that are more larva-like, including open gill stilts until late in development, the curled tips of the distal ceratobranchial III and IV associated with the gill slit, ceratobranchial IV separated until late in development, and a squamosal that is confined to the lateral aspect of the quadrate before it extends to cover the cheek region at, or even after hatching (Müller 2006). In all these respects, embryos of *H. rostratus* are remarkably similar to larvae of fully biphasic caecilians. Thus, considering only Seychelles caecilian species, it seems plausible that free-living larvae have re-evolved in some (San Mauro et al. 2014) by a re-elaboration of larval traits that were retained in a direct-developing ancestor (and maintained in *H. rostratus*) as suggested for *Desmognathus* salamanders (Kerney et al. 2012). However, the great degree of developmental repatterning seen in both *I. russeli* and G. *ramaswamii* may cast doubt on this scenario. Taken at face value, the scenario suggests evolution of a more derived form of direct development (i.e., without retention of larval traits) in ancestral indotyphlids thereby obfuscating any explanation for the presence of free-living larvae in Seychelles indotyphlids. It is possible that larval morphological traits were retained in the direct-developing last common ancestor of Indotyphlidae and then lost independently in the lineages of *I. russeli* and *G. ramaswamii*, but developmental data for additional indotyphlid and non-indotyphlid caecilians are necessary to address this question. In particular, data on the phylogenetic position and development of the Ethiopian *Sylvacaecilia grandisonae* are needed; this species has been classified in Indotyphlidae (Wilkinson et al. 2011) and is the only non-Seychelles teresomatan caecilian that has a free-living larval stage. And last, a better phylogenetic resolution of the Seychelles caecilian taxa will inform our understanding of caecilian life history evolution.

Acknowledgements We thank Katja Felbel for the expert preparation of histological sections and Paul Lukas for advice regarding three-dimensional reconstructions using Amira and Autodesk Maya. The

fieldwork for collection of *Idiocranium* was funded primarily by the US Fish and Wildlife's Wildlife Without Borders, along with several other programs—viz., Amphibians in Decline, Zoological Society of London's EDGE Fellowship, Conservation International's Lost Amphibians, and The Royal Geographical Society—all of which we gratefully acknowledge. This research was funded by a German Research Foundation grant (DFG MU2914/2-1) to HM. DJG and MW are indebted to many Cameroonian people of Mamfe Division who helped us with logistics and generously provided field assistance and hospitality. We thank the people of the villages of Tinta, particularly Tata Eric Tunda, Wilfred, and Rafael (Tinta). We also thank Echalle S. Ndeme and Gespo for looking after us in the field, and Tom Doherty-Bone, Nono Gonwouo, Ngane Benjamin Kome, and Marcel Kouete for their help and support. This manuscript was improved by comments from an anonymous reviewer, which is gratefully acknowledged.

Compliance with ethical standards

Ethical approval All applicable international, national, and institutional guidelines for the collection and use of animals were followed.

References

Alberch P, Gould SJ, Oster GF, Wake DB (1979) Size and shape in ontogeny and phylogeny. Paleobiol 5:296–317

Billo R, Wake MH (1987) Tentacle development in *Dermophis mexicanus* (Amphibia, Gymnophiona) with a hypothesis of tentacle origin. J Morphol 192:101–110

Bonett RM, Mueller RL, Wake DB (2005) Why should reacquisition of larval stages by desmognathine salamanders surprise us? Herpetol Rev 36:112–113

Brauer A (1899) Beitrage zur Kenntniss der Entwicklung und Anatomie der Gymnophionen. II. Die Entwicklung der äusseren Form. Zool Jahrb Abt Anat Ontog Tiere 12:477–508

Bruce RC (2005) Did *Desmognathus* salamanders reinvent the larval stage? Herpetol Rev 36:107–112

Chippindale PT, Wiens JJ (2005) Re-evolution of the larval stage in the plethodontid salamander genus *Desmognathus*. Herpetol Rev 36:113–117

Chippindale PT, Bonett RM, Baldwin AS, Wiens JJ (2004) Phylogenetic evidence for a major reversal of life-history evolution in plethodontid salamanders. Evolution 58:2809–2822

de Bakker DM, Wilkinson M, Jensen B (2015) Extreme variation in the atrial septation of caecilians (Amphibia: Gymnophiona). J Anat 226:1–12

Duellman WE (2015) Marsupial frogs: *Gastrotheca* and allied genera. Johns Hopkins University Press, Baltimore

Duellman WE, Trueb L (1986) Biology of amphibians. McGraw-Hill, New York

Duellman WE, Maxson LR, Jesiolowski CA (1988) Evolution of marsupial frogs (Hylidae: Hemiphractinae): immunological evidence. Copeia 1988:527–543

Dünker N, Wake MH, Olson WM (2000) Embryonic and larval development in the caecilian *Ichthyophis kohtaoensis* (Amphibia, Gymnophiona): a staging table. J Morphol 243:3–34

Dunn ER (1942) The American caecilians. Bull Mus Comp Zool Harvard 91:439–540

Eifertinger L (1933) Die Entwicklung des knöchernen Unterkiefers von *Hypogeophis*. Z Anat Entwicklungsgesch 101:534–552

Frost DR (2018) Amphibian Species of the World: an Online Reference. Version 6.0. Electronic Database accessible at http://research.amnh.org/herpetology/ amphibia/index.html. American Museum of Natural History, New York, USA. Accessed 06 Sept 2018

Gower DJ, Giri V, Dharne MS, Shouche YS (2008) Frequency of independent origins of viviparity among caecilians (Gymnophiona): evidence from the first 'live-bearing' Asian amphibian. J Evol Biol 21:1220–1226

Gower DJ, Kouete MT, Doherty-Bone TM, Ndeme ES, Wilkinson M (2015) Rediscovery, natural history, and conservation status of *Idiocranium russeli* Parker, 1936 (Amphibia: Gymnophiona: Indotyphlidae). J Nat Hist 49:233–253

Hanken J (2003) Direct development. In: Hall BK, Olson WM (eds) Keywords and concepts in evolutionary developmental biology. Harvard University Press, Cambridge, pp 97–102

Hanken J, Wake DB (1993) Miniaturization of body size: organismal consequences and evolutionary significance. Annu Rev Ecol Syst 24:501–519

Himstedt W (1996) Die Blindwühlen. Westarp Wissenschaften, Magdeburg

Kamei RG, San Mauro D, Gower DJ, Van Bocxlaer I, Sherratt E, Thomas A, Babu S, Bossuyt F, Wilkinson M, Biju SD (2012) Discovery of a new family of amphibians from northeast India with ancient links to Africa. Proc R Soc B 279:2396–2401

Kerney RR, Blackburn DC, Müller H, Hanken J (2012) Do larval traits re-evolve? Evidence from the embryogenesis of a direct-developing salamander, *Plethodon cinereus*. Evolution 66:252–262

Kleinteich T (2009) The evolution of intrauterine feeding in the Gymnophiona (Lissamphibia): a comparative study on the morphology, function, and development of cranial muscles in oviparous and viviparous species. Dissertation, University of Hamburg

Kleinteich T, Haas A (2007) Cranial musculature in the larva of the caecilian, *Ichthyophis kohtaoensis* (Lissamphibia: Gymnophiona). J Morphol 268:74–88

Kleinteich T, Haas A (2011) The hyal and ventral branchial muscles in caecilian and salamander larvae: homologies and evolution. J Morphol 272:598–613

Krings M, Müller H, Heneka M, Rödder D (2017) Modern morphological methods for tadpole studies. A comparison of micro-CT, and clearing and staining protocols modified for frog larvae. Biotech Histochem 92:595–605

Liedtke HC, Müller H, Hafner J, Penner J, Gower DJ, Mazuch T, Rödel M-O, Loader SP (2017) Terrestrial reproduction as an adaptation to steep terrain in African toads. Proc R Soc B 284:20162598

Maddin HC, Russell AP, Anderson JS (2012) Phylogenetic implications of the morphology of the braincase of caecilian amphibians (Gymnophiona). Zool J Linn Soc 166:160–201

Maddock ST, Wilkinson M, Gower DJ (2018) A new species of small, long-snouted *Hypogeophis* Peters, 1880 (Amphibia: Gymnophiona: Indotyphlidae) from the highest elevations of the Seychelles island of Mahé. Zootaxa 4450:359–375

Magnusson WE, Hero JM (1991) Predation and the evolution of complex oviposition behaviour in Amazon rainforest frogs. Oecologia 86:310–318

Marcus H (1933) Zur Entstehung des Unterkiefers von *Hypogeophis*. Beitrag zur Kenntnis der Gymnophionen XX. Anat Anz 77:178–184

Marcus H, Stimmelmayr E, Porsch G (1935) Die Ossifikation des Hypogeophisschädels. Beitrag zur Kenntnis der Gymnophionen XXV. Gegenbaurs Morphol Jb 76:375–420

Milner AR (1988) The relationships and origin of living amphibians. In: Benton MJ (ed) The phylogeny and classification of the tetrapods. Clarendon Press, Oxford, pp 59–102

Mueller RL, Macey JR, Jaekel M, Wake DB, Boore JL (2004) Morphological homoplasy, life history evolution, and historical biogeography of plethodontid salamanders inferred from complete mitochondrial genomes. PNAS 101:13820–13825

Mulisch M, Welsch U (2015) Romeis—Mikroskopische Technik. Springer, Heidelberg

Müller H (2006) Ontogeny of the skull, lower jaw, and hyobranchial skeleton of *Hypogeophis rostratus* (Amphibia: Gymnophiona: Caeciliidae) revisited. J Morphol 267:968–986

Müller H (2007) Developmental morphological diversity in caecilian amphibians: systematic and evolutionary implications. Dissertation, Leiden University Press

Müller H, Oommen OV, Bartsch P (2005) Skeletal development of the direct-developing caecilian *Gegeneophis ramaswamii* (Amphibia: Gymnophiona: Caeciliidae). Zoomorphology 124:171–188

Müller H, Wilkinson M, Loader SP, Wirkner CS, Gower DJ (2009) Morphology and function of the head in foetal and juvenile *Scolecomorphus kirkii* (Amphibia: Gymnophiona: Scolecomorphidae). Biol J Linn Soc 96:491–504

Müller H, Liedtke HC, Menegon M, Beck J, Balesteros L, Nagel P, Loader SP (2013) Forests as promoters of terrestrial life-history strategies in East African amphibians. Biol Lett 9:20121146

Nussbaum RA (1983) The evolution of a unique dual jaw-closing mechanism in caecilians: (Amphibia: Gymnophiona) and its bearing on caecilian ancestry. J Zool 199:545–554

Nussbaum RA (1984) Amphibians of the Seychelles. In: Stoddart DR (ed) Biogeography and ecology of the Seychelles islands. Dr. W. Junk Publishers, The Hague, pp 379–415

Nussbaum RA, Naylor BG (1982) Variation in the trunk musculature of caecilians (Amphibia: Gymnophiona). J Zool 198:383–398

Parker HW (1936) The Amphibians of the Mamfe Division, Cameroons. I. Zoogeography and systematics. Proc Zool Soc Lond 106:135–163

Parker HW (1958) Caecilians of the Seychelles islands with description of a new subspecies. Copeia 1958:71–76

Parsons TS, Williams EE (1963) The relationships of the modern Amphibia: a re-examination. Q Rev Biol 38:26–53

Pérez OD, Lai NB, Buckley D, del Pino EM, Wake MH (2009) The morphology of prehatching embryos of *Caecilia orientalis* (Amphibia: Gymnophiona: Caeciliidae). J Morphol 270:1492–1502

Peter K (1898) Die Entwicklung und funktionelle Gestaltung des Schädels von *Ichthyophis glutinosus*. Morphol Jb 25:555–628

Reilly SM, Wiley EO, Meinhardt DJ (1997) An integrative approach to heterochrony: the distinction between interspecific and intraspecific phenomena. Biol J Linn Soc 60:119–143

San Mauro D (2010) A multilocus timescale for the origin of extant amphibians. Mol Phylogenet Evol 56:554–561

San Mauro D, Gower DJ, Müller H, Loader SP, Zardoya R, Nussbaum RA, Wilkinson M (2014) Life-history evolution and mitogenomic phylogeny of caecilian amphibians. Mol Phylogenet Evol 73:177–189

Sanderson IT (1937) Animal treasure. Viking Press, New York

Schweiger S, Naumann B, Larson JG, Möckel L, Müller H (2017) Direct development in African squeaker frogs (Anura: Arthroleptidae: *Arthroleptis*) reveals a mosaic of derived and plesiomorphic characters. Org Divers Evol 17:693–707

Szarski H (1962) The origin of the Amphibia. Q Rev Biol 37:189–241

Taylor EH (1969) Skulls of Gymnophiona and their significance in the taxonomy of the group. Kans Univ Sci Bull 48:585–687

Todd BD (2007) Parasites lost? An overlooked hypothesis for the evolution of alternative reproductive strategies in amphibians. Am Nat 170:7793–7799

Visser MHC (1963) The cranial morphology of *Ichthyophis glutinosus* (Linné) and *Ichthyophis monochrous* (Bleeker). Ann Univ Stellenbosch 38:67–102

Wake MH (1977) The reproductive biology of caecilians: an evolutionary perspective. In: Taylor EH, Guttman SI (eds) The reproductive biology of amphibians. Plenum Press, New York, pp 73–101

Wake MH (1986) The morphology of *Idiocranium russeli* (Amphibia: Gymnophiona), with comments on miniaturization through heterochrony. J Morphol 189:1–16

Wake MH (2003) The osteology of caecilians. In: Heatwole H (ed) Amphibian biology. Osteology, vol 5. Surrey Beatty and Sons, Chipping Norton, pp 1809–1876

Wake MH, Hanken J (1982) Development of the skull of *Dermophis mexicanus* (Amphibia: Gymnophiona), with comments on skull kinesis and amphibian relationships. J Morphol 173:203–223

Wake DB, Hanken J (1996) Direct development in the lungless salamanders: what are the consequences for developmental biology, evolution and phylogenesis? Int J Dev Biol 40:859–869

Wiens JJ, Kuczynski CA, Duellman WE, Reeder TW (2007) Loss and re-evolution of complex life cycles in marsupial frogs: does ancestral trait reconstruction mislead? Evolution 61:1886–1899

Wilkinson M (2012) Caecilians. Curr Biol 22:668–669

Wilkinson M, Nussbaum RA (1997) Comparative morphology and evolution of the lungless caecilian *Atretochoana eiselti* (Taylor) (Amphibia: Gymnophiona: Typhlonectidae). Biol J Linn Soc 62:39–109

Wilkinson M, San Mauro D, Sherratt E, Gower DJ (2011) A nine-family classification of caecilians (Amphibia: Gymnophiona). Zootaxa 2874:41–64